

Atomic Scale Investigations of Interfacial Line Defects

Douglas L. Medlin

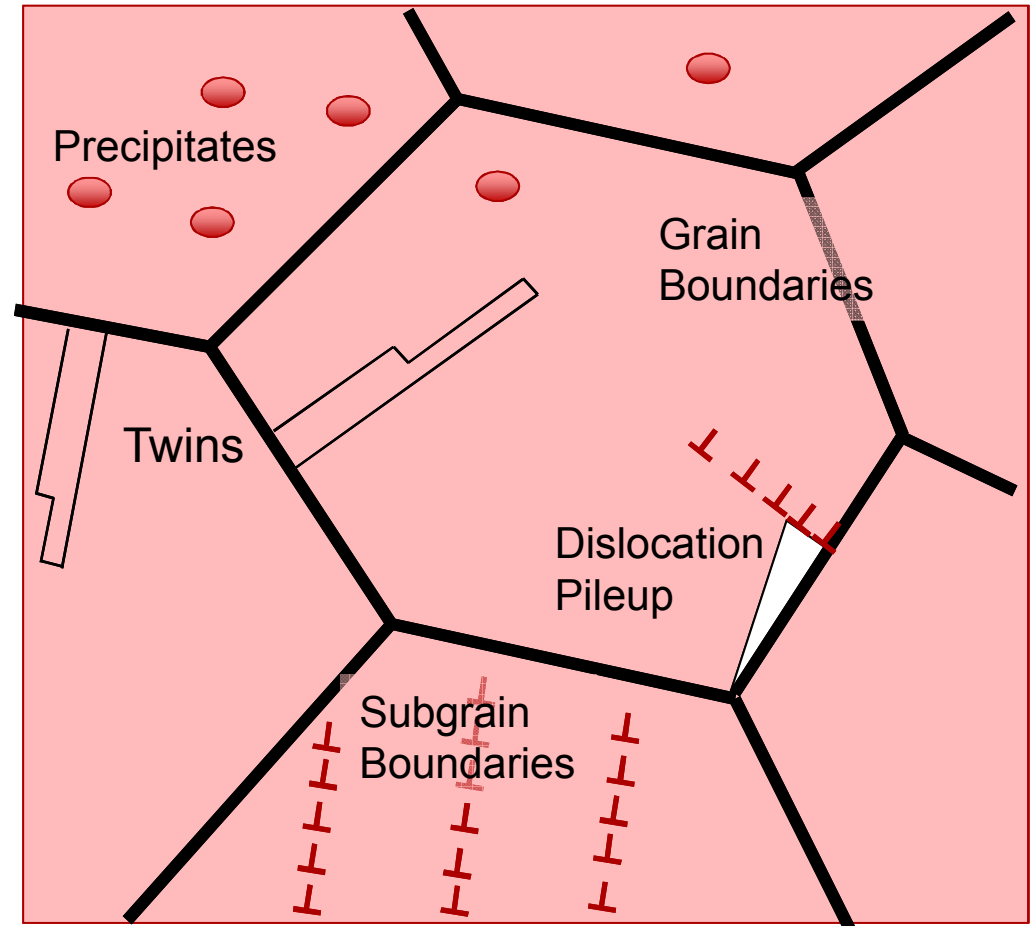
Sandia National Laboratories, Livermore, CA

dlmedli@sandia.gov

Interfaces:

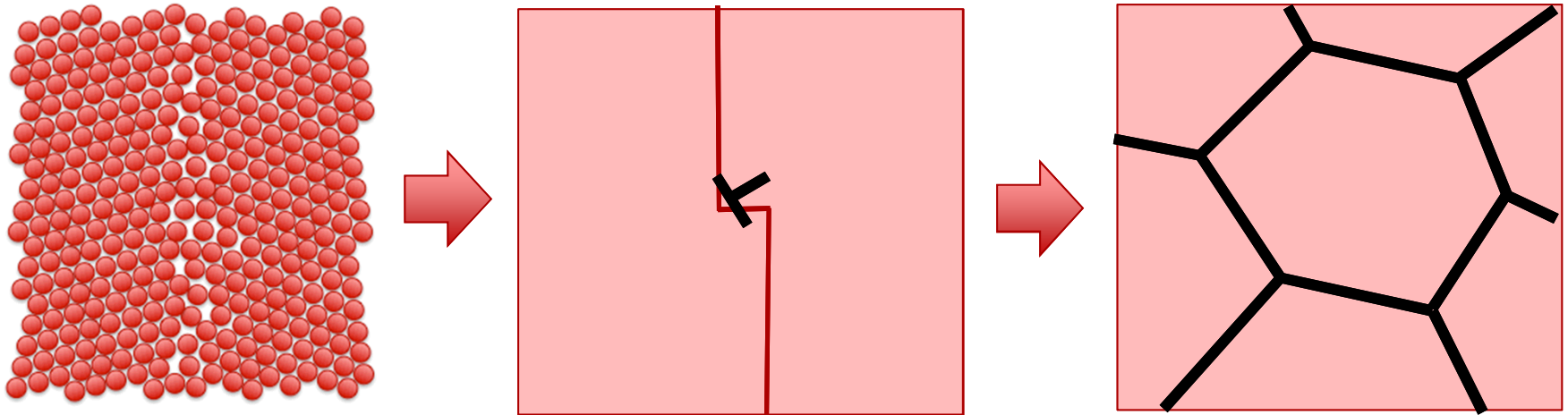
Central to materials properties and behavior

- Barriers to slip.
 - Hardening.
 - Stress concentration
- Softening at high T.
 - e.g., gb sliding, creep
- Sinks for point defects, dislocations
 - e.g. recrystallization
- Heterogeneous nucleation sites
- Compositional segregation, diffusional pathways.
- Electronic and Thermal transport



Interfacial Line Defects:

An important bridging concept

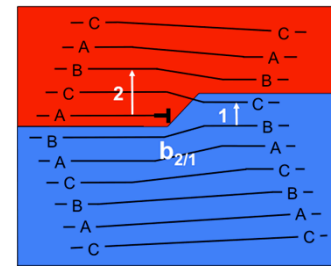
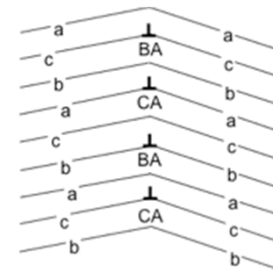


- **Connection between details of atomic structure and larger-scale materials properties.**
- **Essential to extending from specific boundaries to more general boundaries**
- **Provide clues to essential physics and mechanisms controlling behavior and properties of interfaces.**

Outline

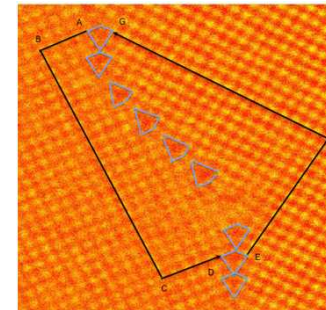
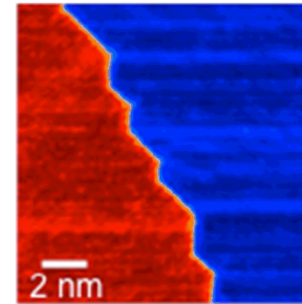
Background on Interfacial Line defects

- Overview of defect types
- Examples from low and high angle GBs.



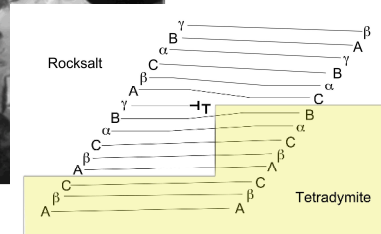
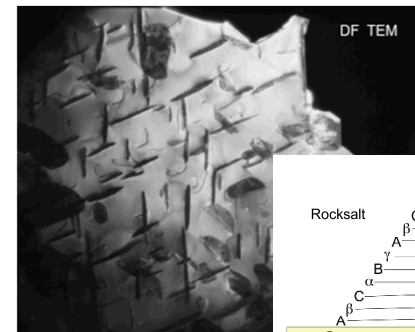
GB disconnections and facet junctions

- Asymmetric $\Sigma=5$ GB in BCC Fe
- Interplay of facet junctions and grain boundary disconnections



Disconnections at heterophase interfaces

- Telluride precipitates in thermoelectric alloy.
- Role of disconnections in transformation mechanism and interfacial strain relief.



Acknowledgements

Sandia/CA

J.D. Sugar

J.A. Zimmerman

Sandia/NM

F. Abdeljawad

K. Hattar

S.M. Foiles

California Institute of Technology

G.J. Snyder (present address Northwestern University)

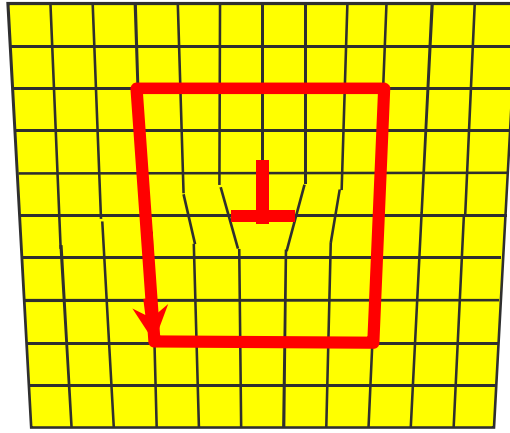
N.A. Heinz

T. Ikeda

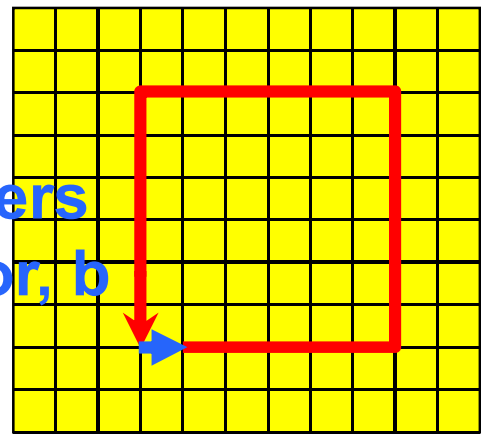
Sandia National Laboratories is a multi-program laboratory managed and operated by Sandia Corporation, a wholly owned subsidiary of Lockheed Martin Corporation, for the U.S. Department of Energy's National Nuclear Security Administration under contract DE-AC04-94AL85000.

Line Defects:

Edge Dislocation

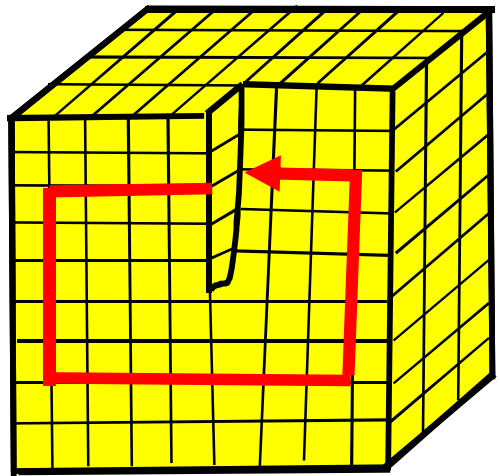


Reference Frame:
Perfect Crystal

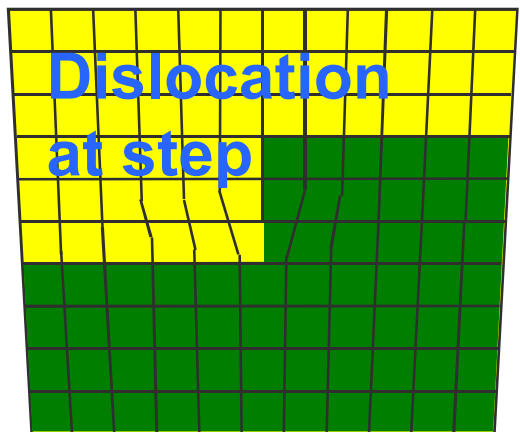
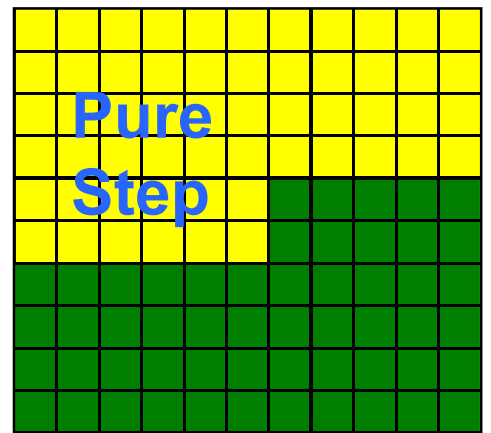


Burgers
Vector, b

Screw Dislocation

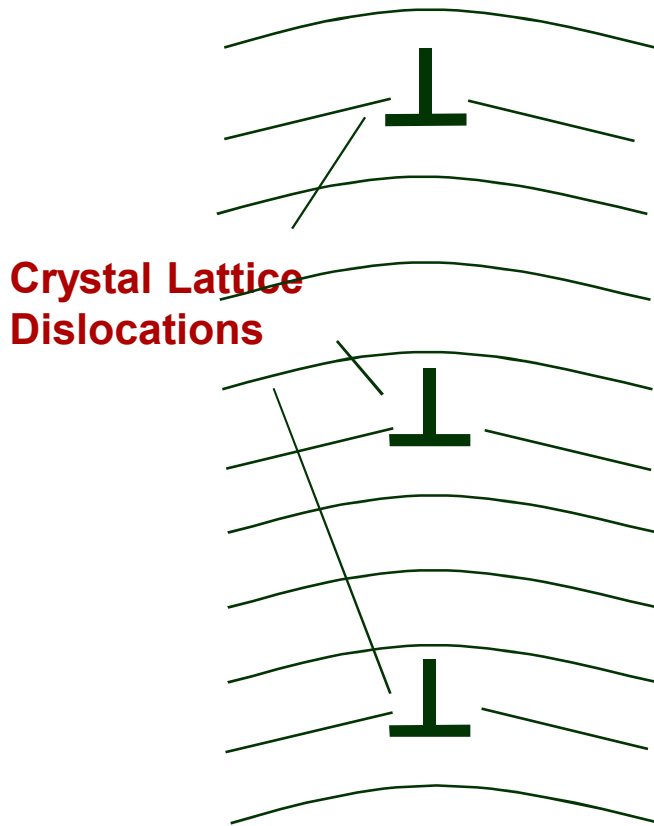


Interfacial Disconnection



Both topological and morphological characteristics are important

Low angle grain boundaries: Arrays of dislocations



Reference Frame:
Single Crystal

**For symmetric tilt
boundaries:**

$$\theta = 2\sin^{-1}(b/2D)$$

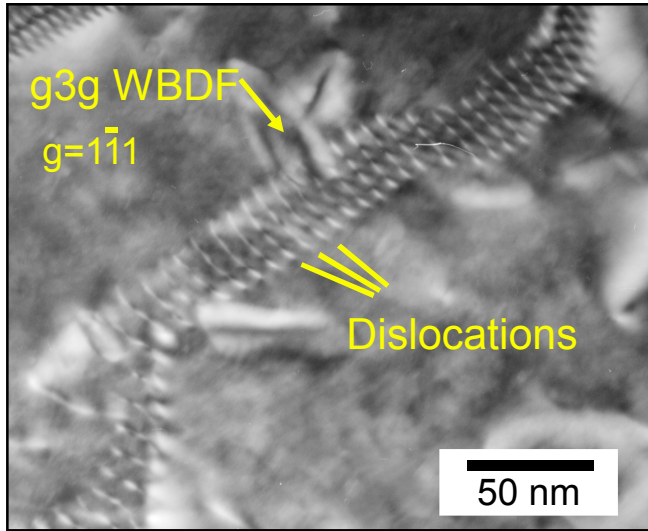
Misorientation

Burgers vector

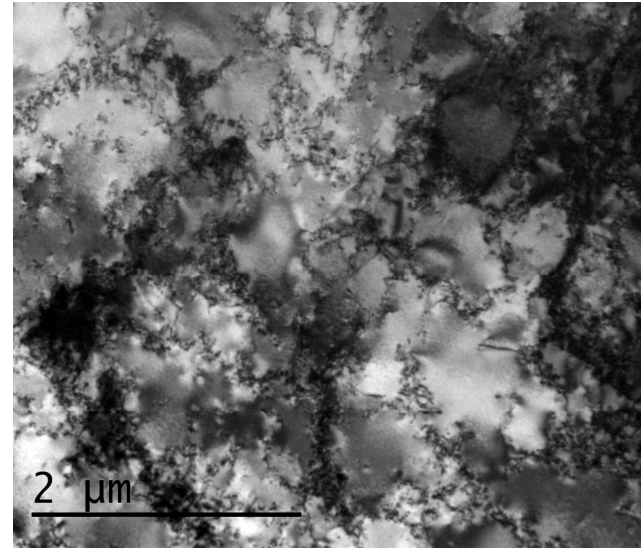
Spacing

Low Angle Grain Boundaries in Various contexts

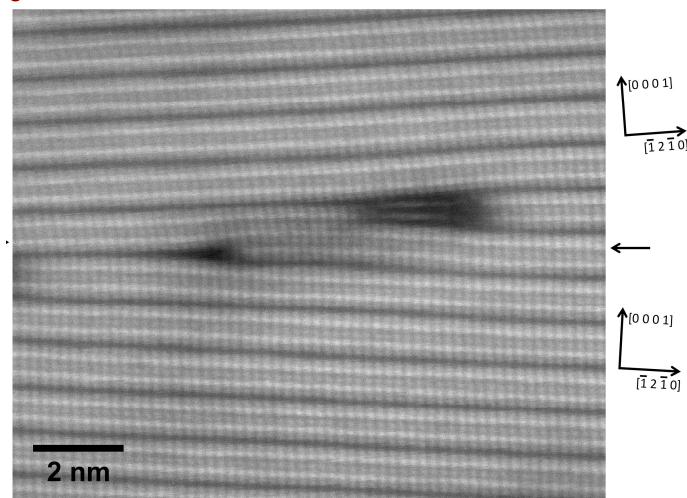
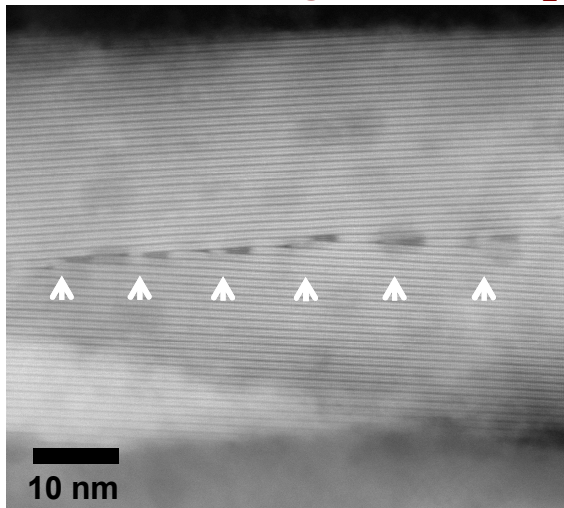
Low angle tilt boundary in Al thin film.



Dislocation Cells in Deformed Ni.



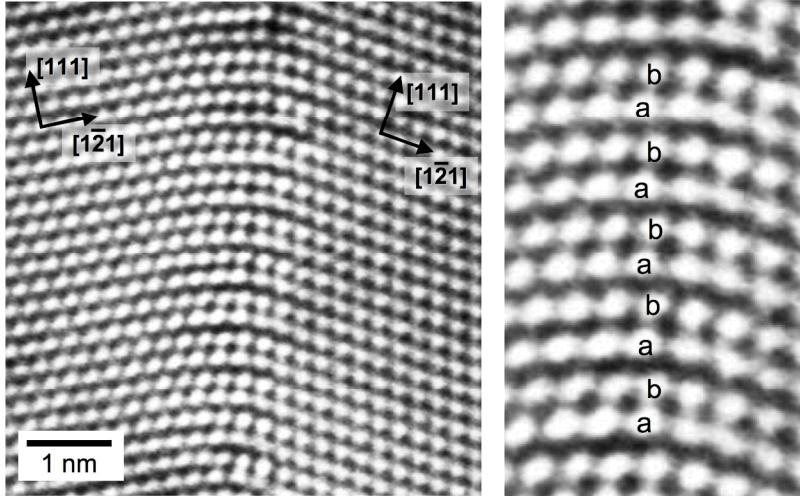
Low Angle GB in Bi_2Te_3 thermoelectric Nanowire



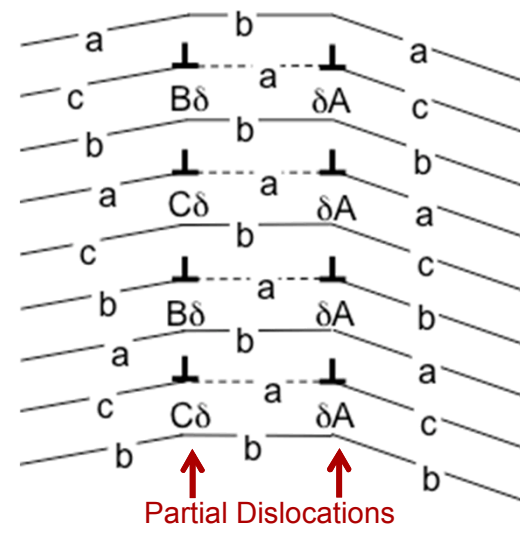
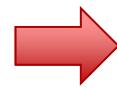
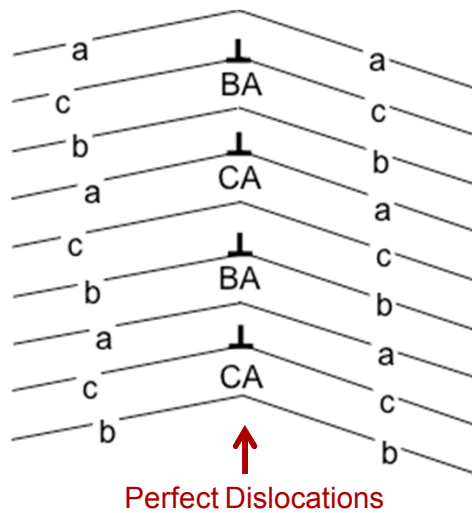
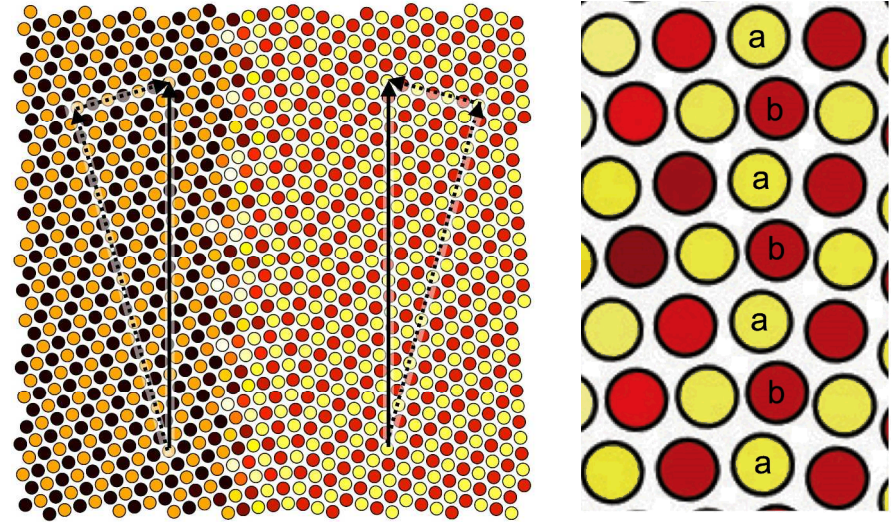
Limit for Low-Angle GBs: Dislocation Core Overlap

An extreme example: HCP Stacking at 29° boundary in Gold

HRTEM



EAM

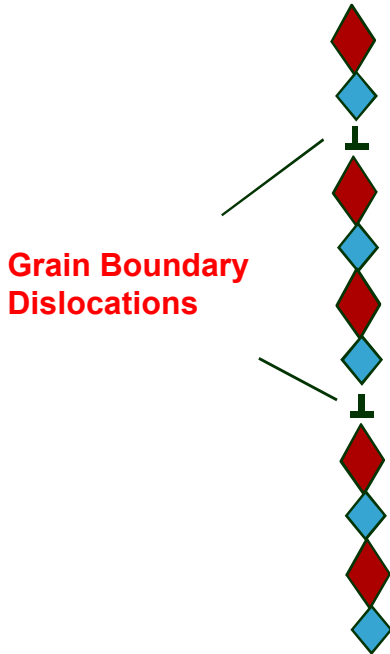


Dissociation into partial dislocations.

Stacking fault every 2 planes gives HCP stacking

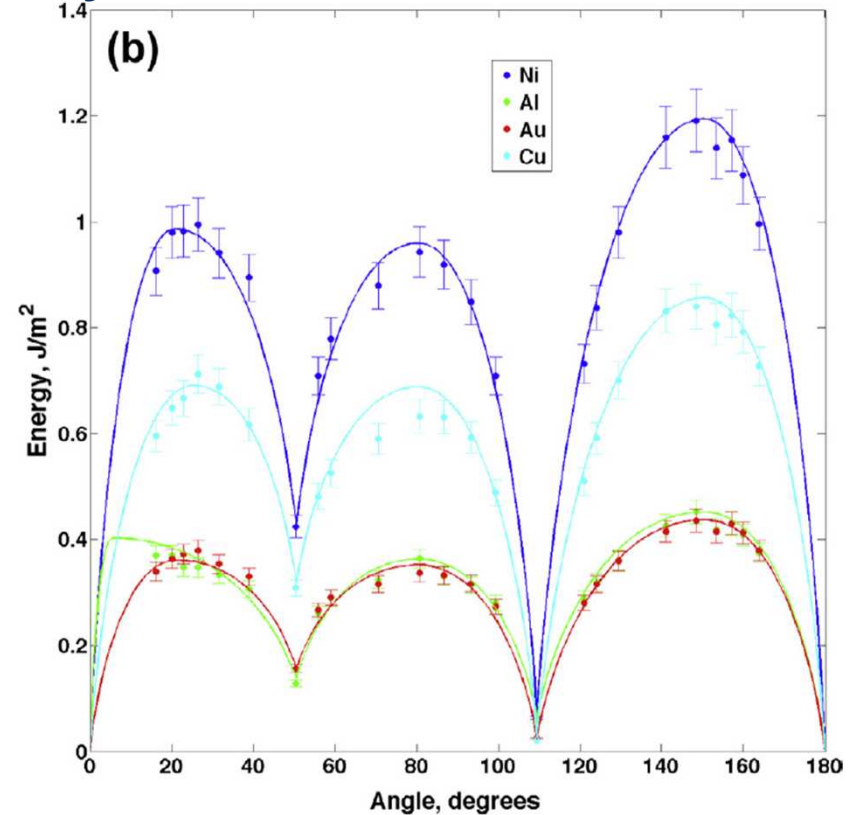
Dislocations in High Angle Boundaries

High Angle GB



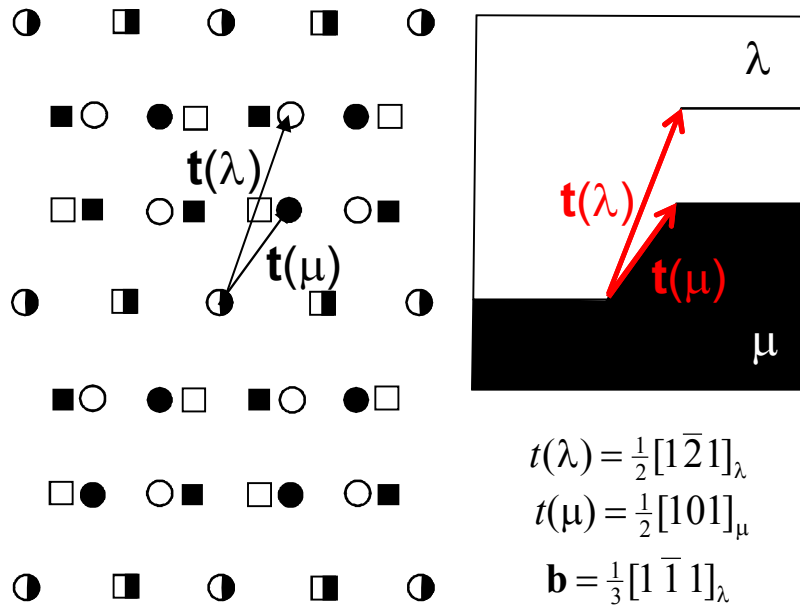
Reference Frame:
Energy Minima in
misorientation/inclination space

Energy vs misorientation Symmetric FCC $\langle 110 \rangle$ tilt boundaries



V.V. Bulatov, B.W. Reed, M. Kumar,
Acta Mat 2014

Interfacial Line defects: in general have both dislocation and step content



Crystal lattice translation vectors

$$\mathbf{b}_{ij} = \mathbf{t}(\lambda)_{ij} - \mathbf{P} \mathbf{t}(\mu)_{ij}$$

Burgers vectors of the set of "admissible" defects

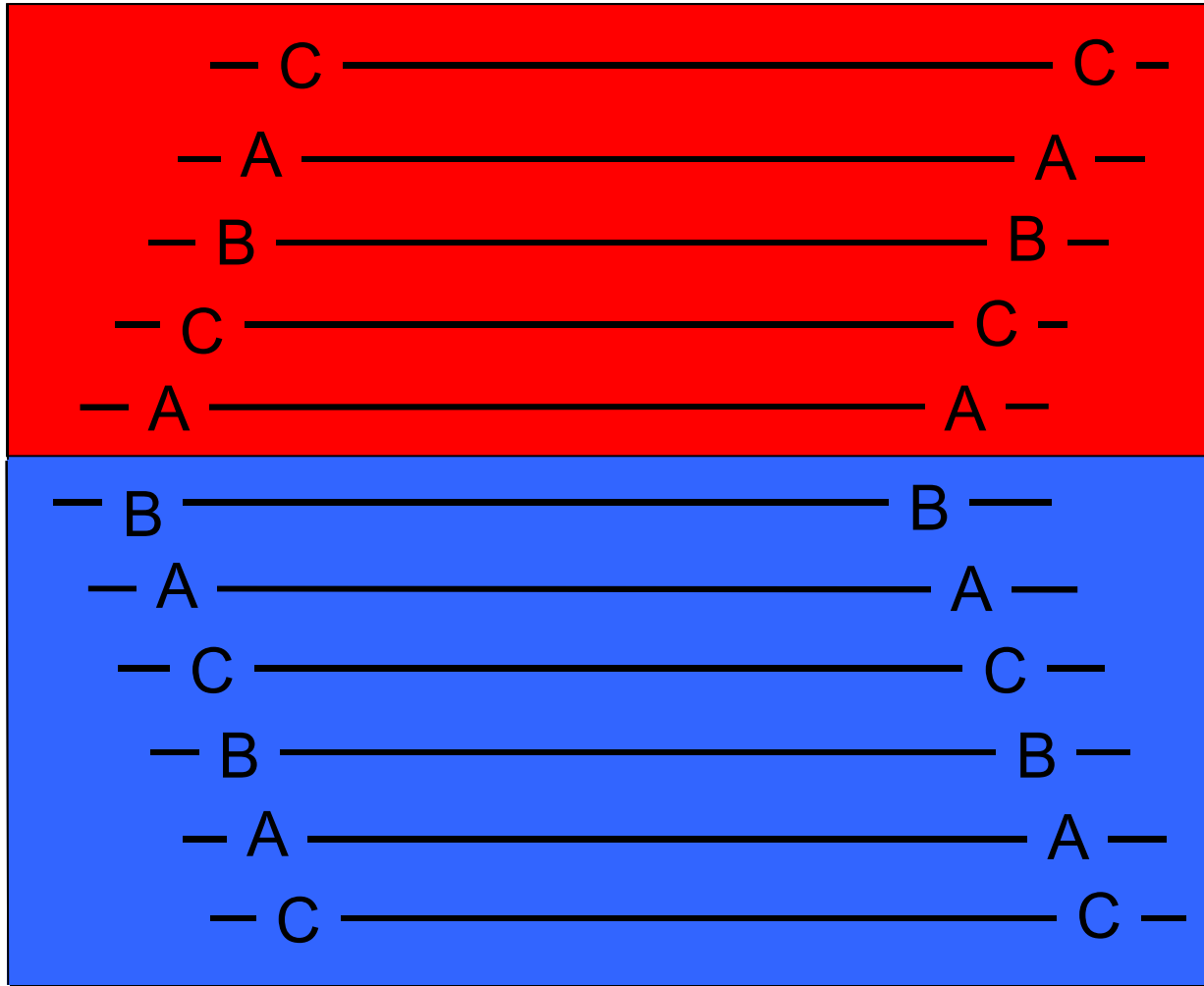
Matrix converts from μ to λ crystal coordinates

"disconnection" = both step and dislocation content

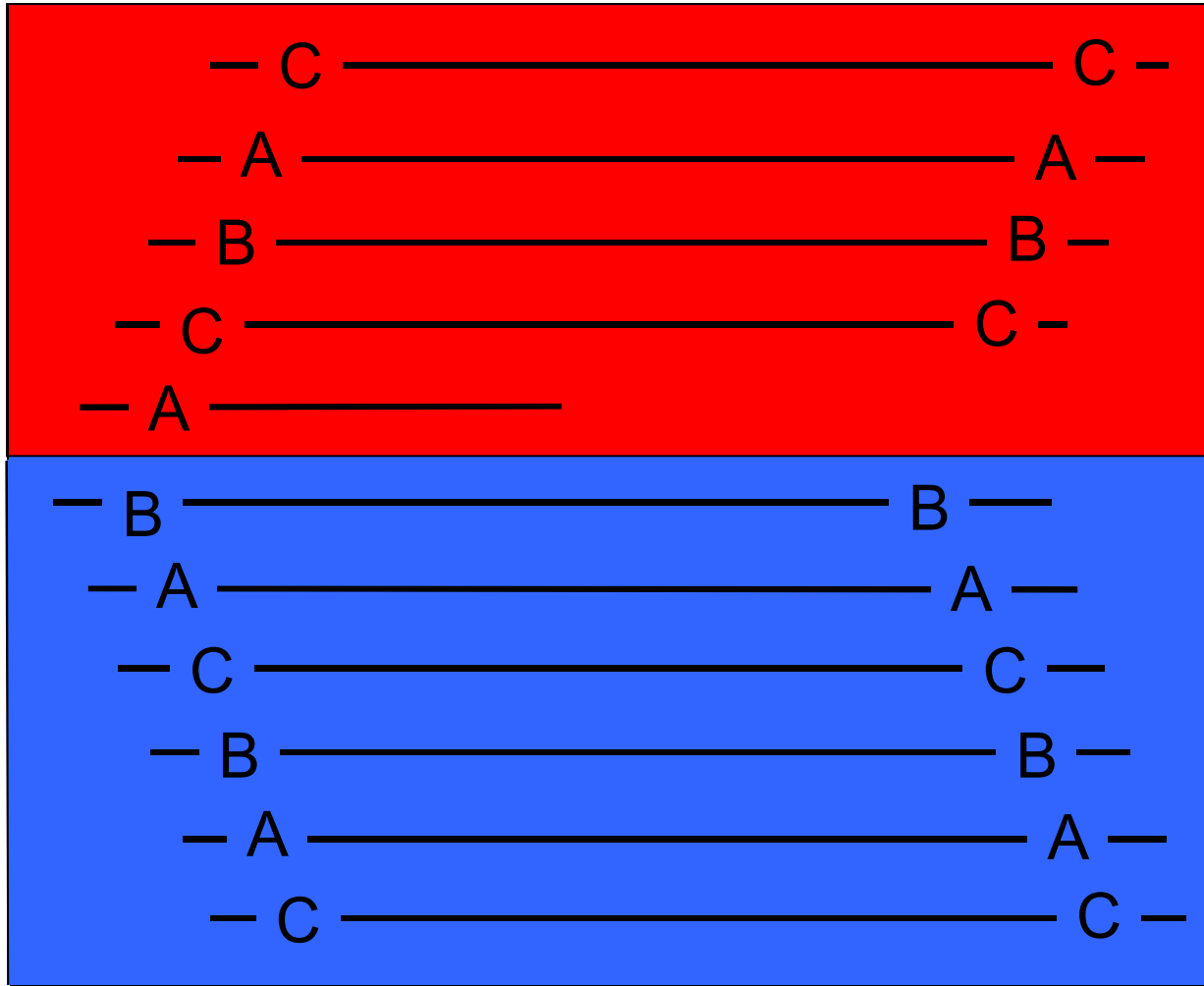
R.C. Pond, Dislocations in Solids, Chapter 38 (1989)

J. Hirth & R.C. Pond, Acta Materialia (1996)

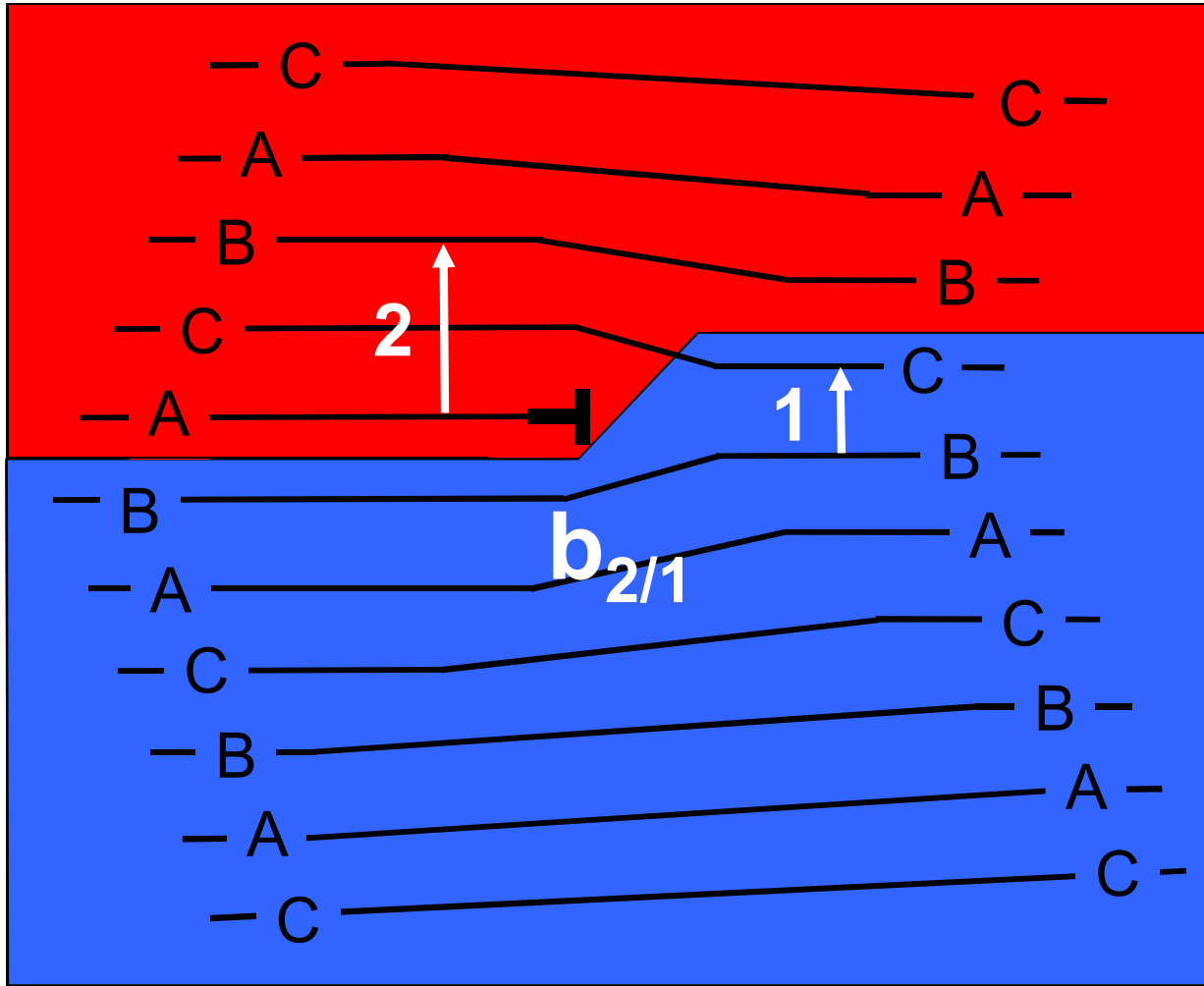
Example: $(1/3)\langle 111 \rangle$ twin disconnections



Example: $(1/3)\langle 111 \rangle$ twin disconnections

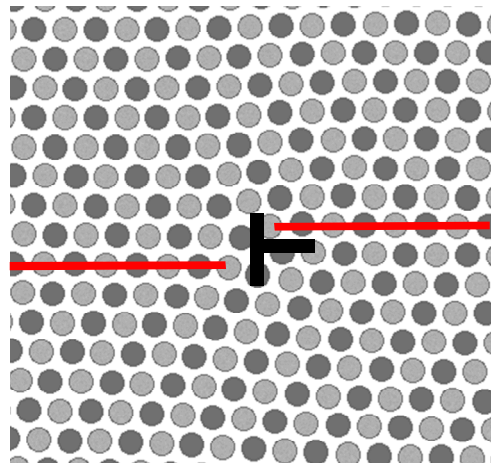
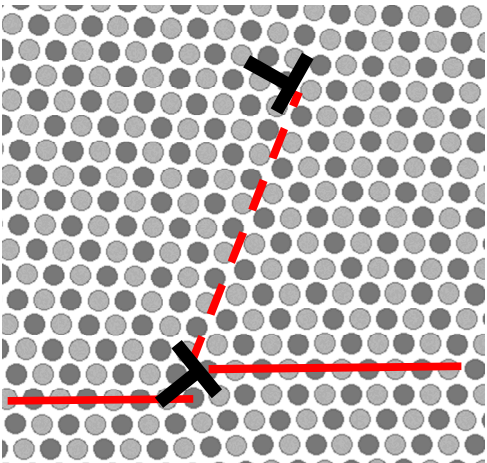
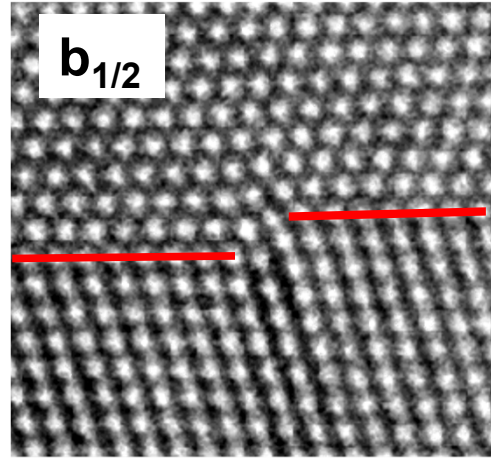
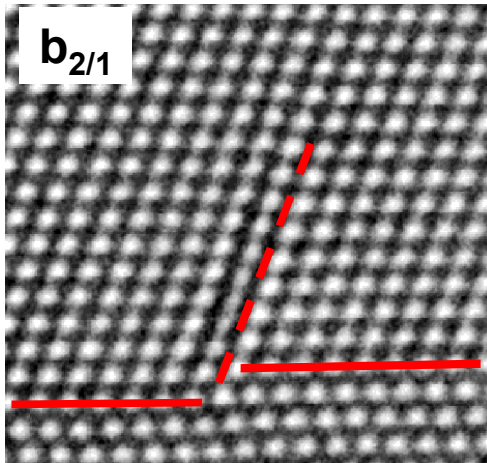


Example: $(1/3)\langle 111 \rangle$ twin disconnections



Example:

$(1/3) \langle 111 \rangle$ Disconnection at twin in Au



- Interface breaks symmetry of dislocation.

- $b_{2/1}$ reduces strain energy by dissociating into Shockley and stair rod dislocations.

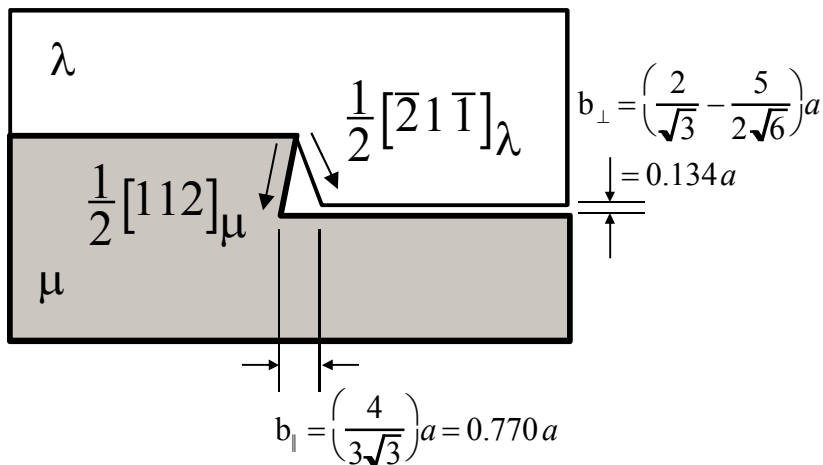
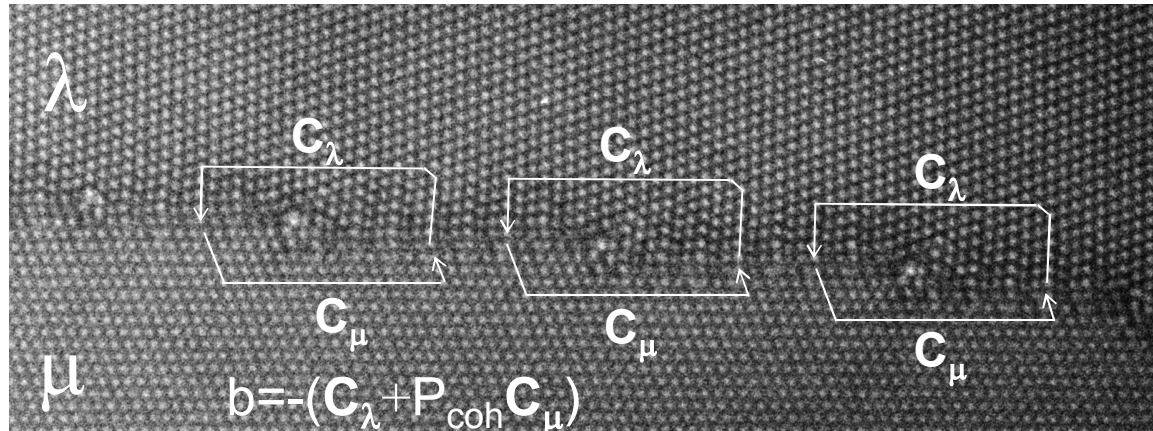
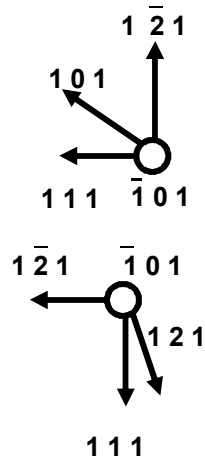
- $b_{1/2}$ disconnection cannot dissociate without creating unfavorable “AA” stacking.

E.A. Marquis and D.L. Medlin,
Phil. Mag. Letters (2005).

← Opposite Burgers Vectors →

Example: Accommodation of Grain Boundary Misfit by Disconnections

90° Boundary in Gold



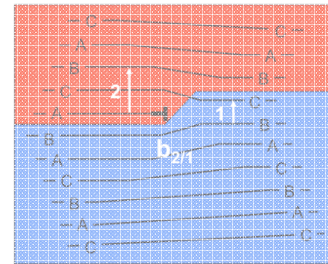
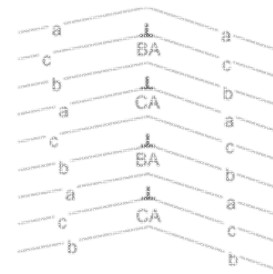
- Coherent reference frame, P_{coh} , describes the 90° rotation of coordinates and strain to bring λ and μ into coherency.
- Defects efficiently accommodate the 5.7% misfit parallel to the $\{111\}/\{112\}$ facets.
- Nearest CSL is $\Sigma=99$

D.L. Medlin, D. Cohen, and R.C. Pond,
Phil. Mag. Letts., 2003.

Outline

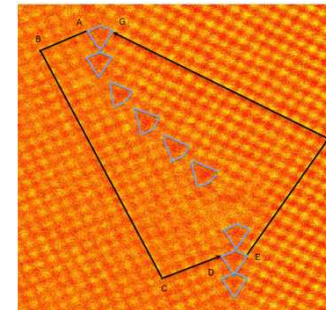
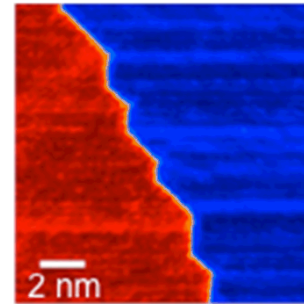
Background on Interfacial Line defects

- Overview of defect types
- Examples from low and high angle GBs.



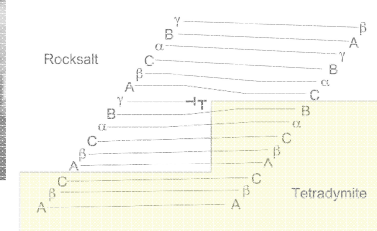
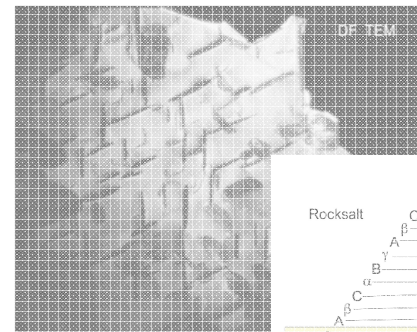
GB disconnections and facet junctions

- Asymmetric $\Sigma=5$ GB in BCC Fe
- Interplay of facet junctions and grain boundary disconnections

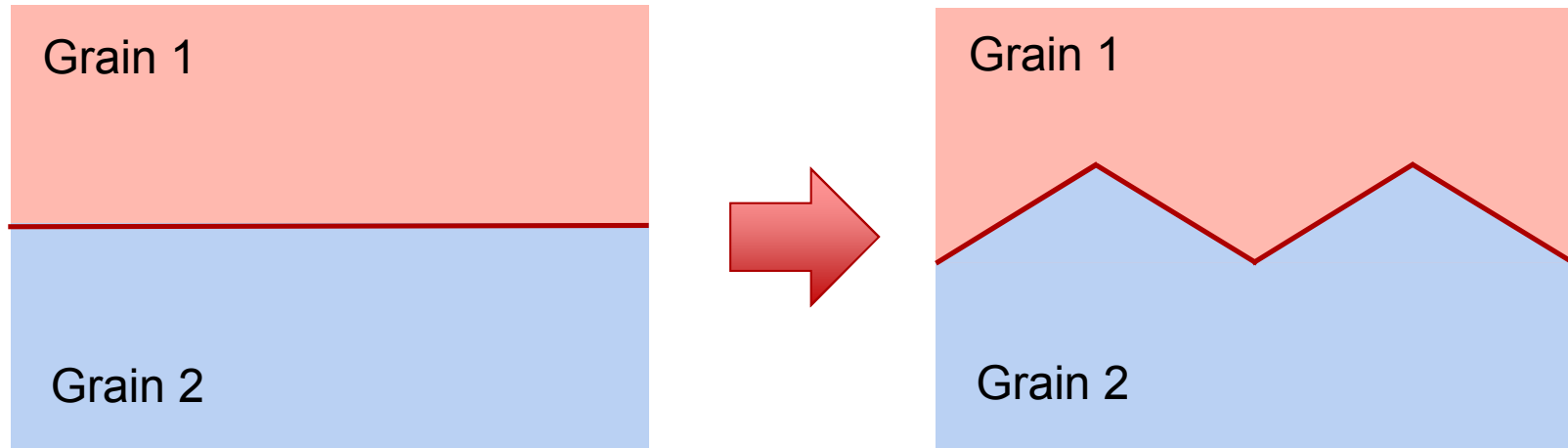


Disconnections at heterophase interfaces

- Telluride precipitates in thermoelectric alloy.
- Role of disconnections in transformation mechanism and interfacial strain relief.



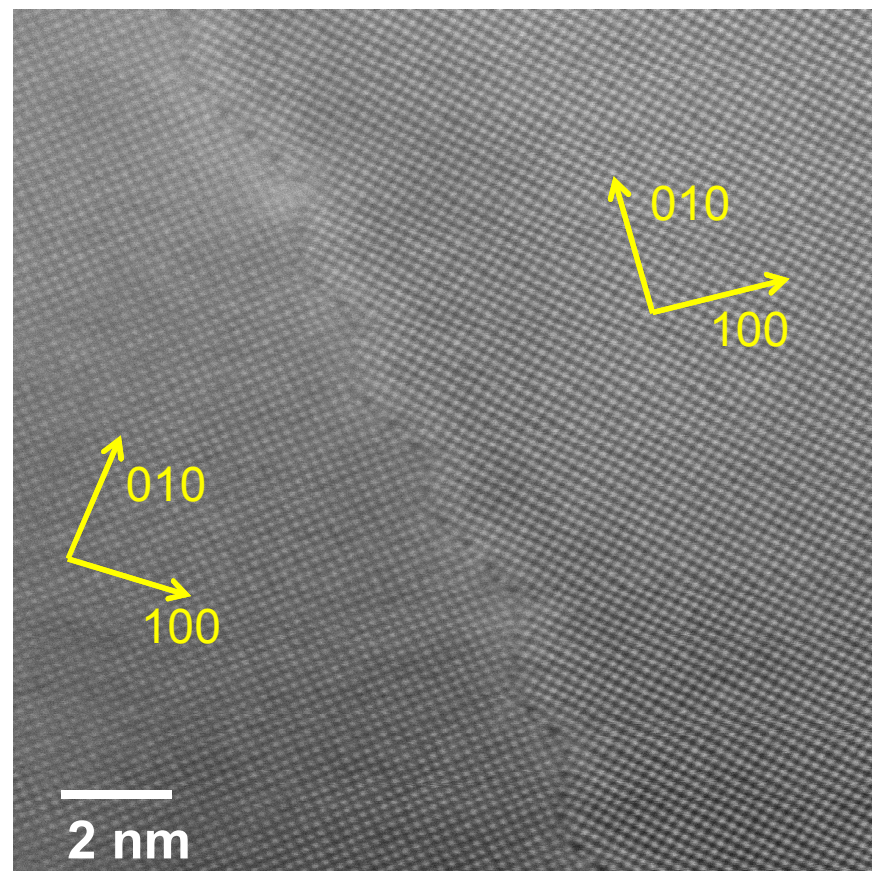
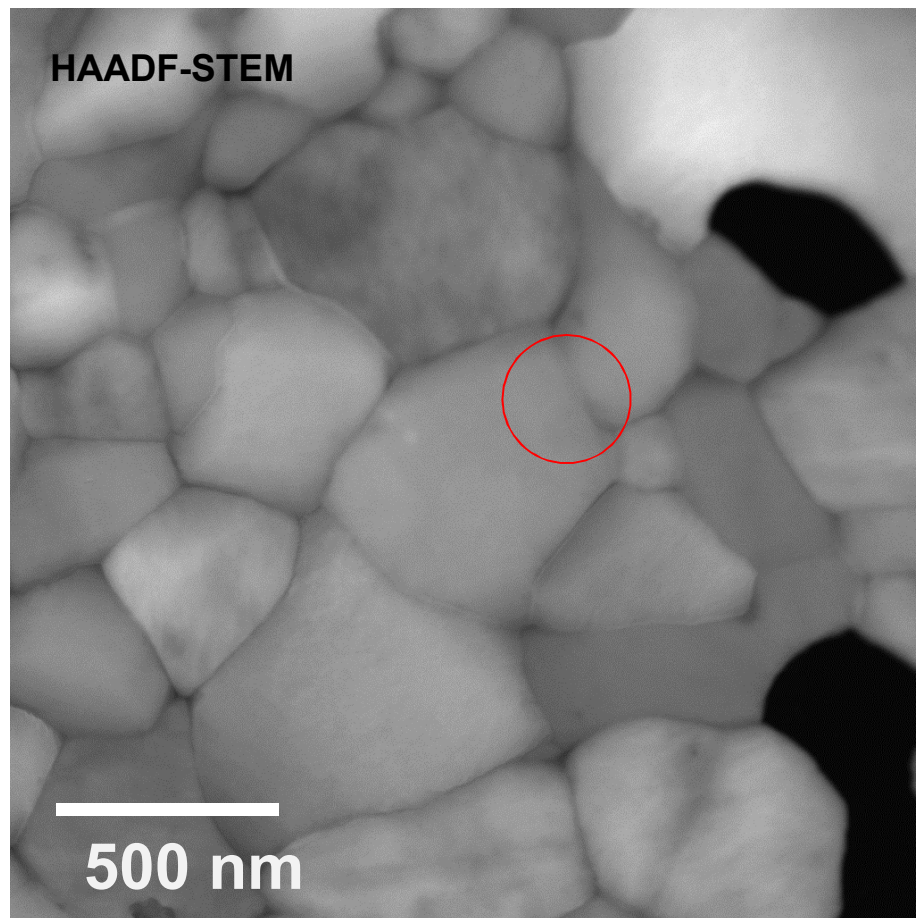
Grain Boundary Faceting



- Reduce interface energy by faceting on lower energy inclinations.
- How do grain boundary dislocations affect the structure of the junctions and the length-scale of the faceting?
- Explore in a faceted $\Sigma=5$ boundary in BCC Fe.

D.L. Medlin, K. Hattar, F. Abdeljawad, J.A. Zimmerman, S.M. Foiles
in preparation for Acta Materialia

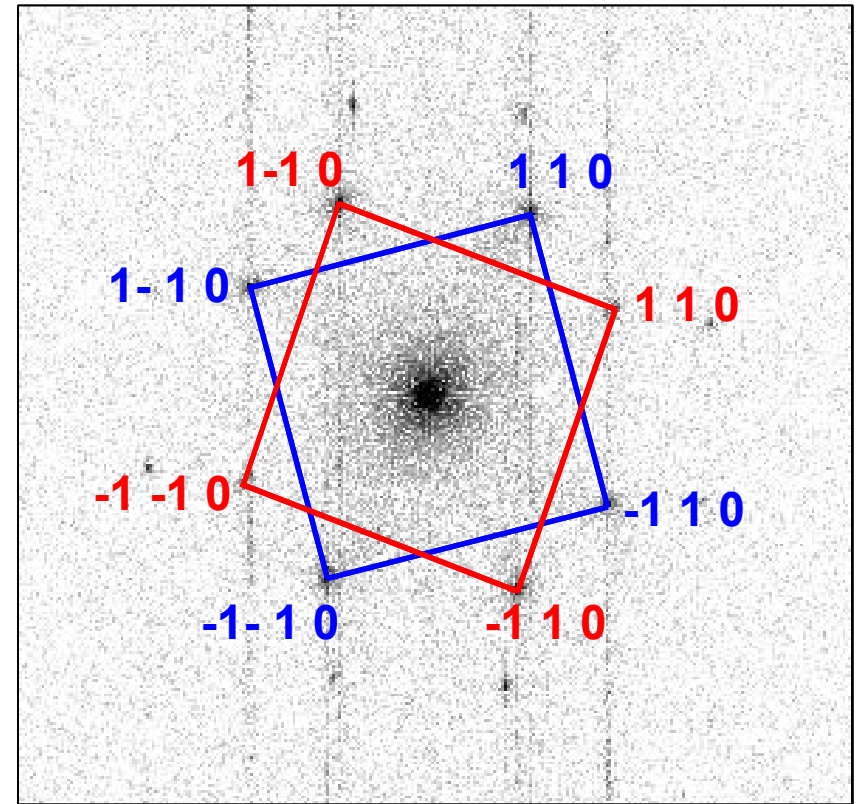
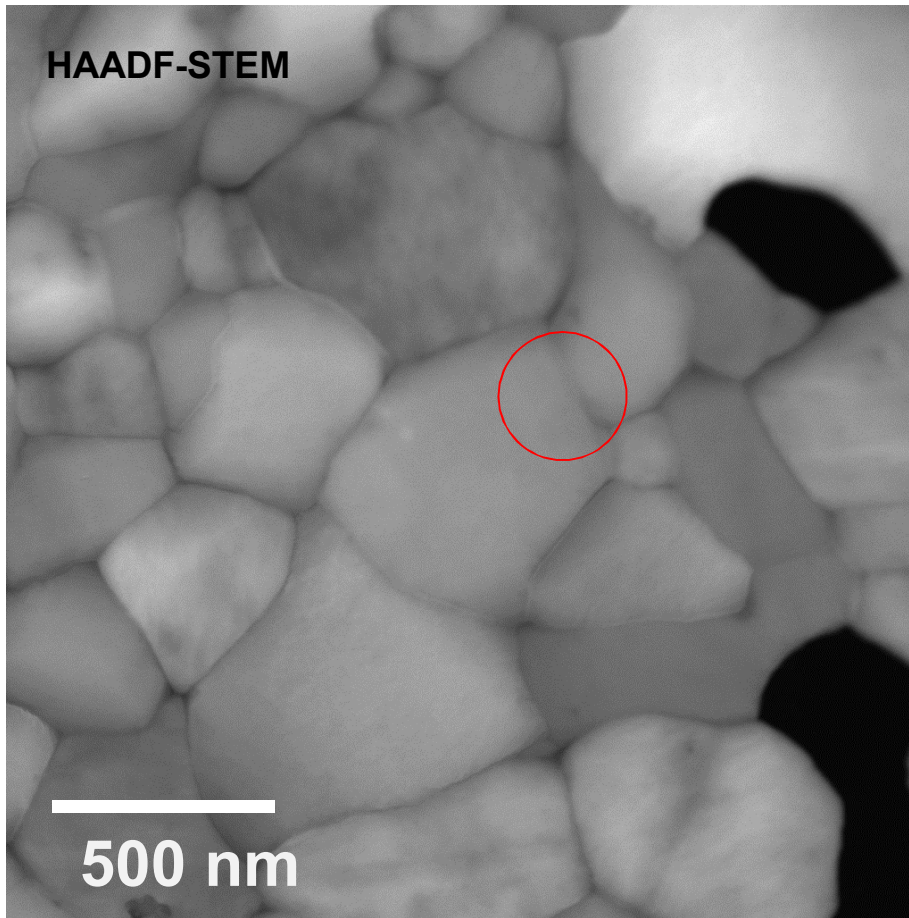
Observations: Polycrystalline BCC Fe film



Pulsed Laser Deposited Fe on Rocksalt (NaCl). 36 nm thickness.
Specimen released and annealed on Mo grid 675°C, 2 hours.
under vacuum

HAADF-STEM
FEI-200 keV probe corrected Titan

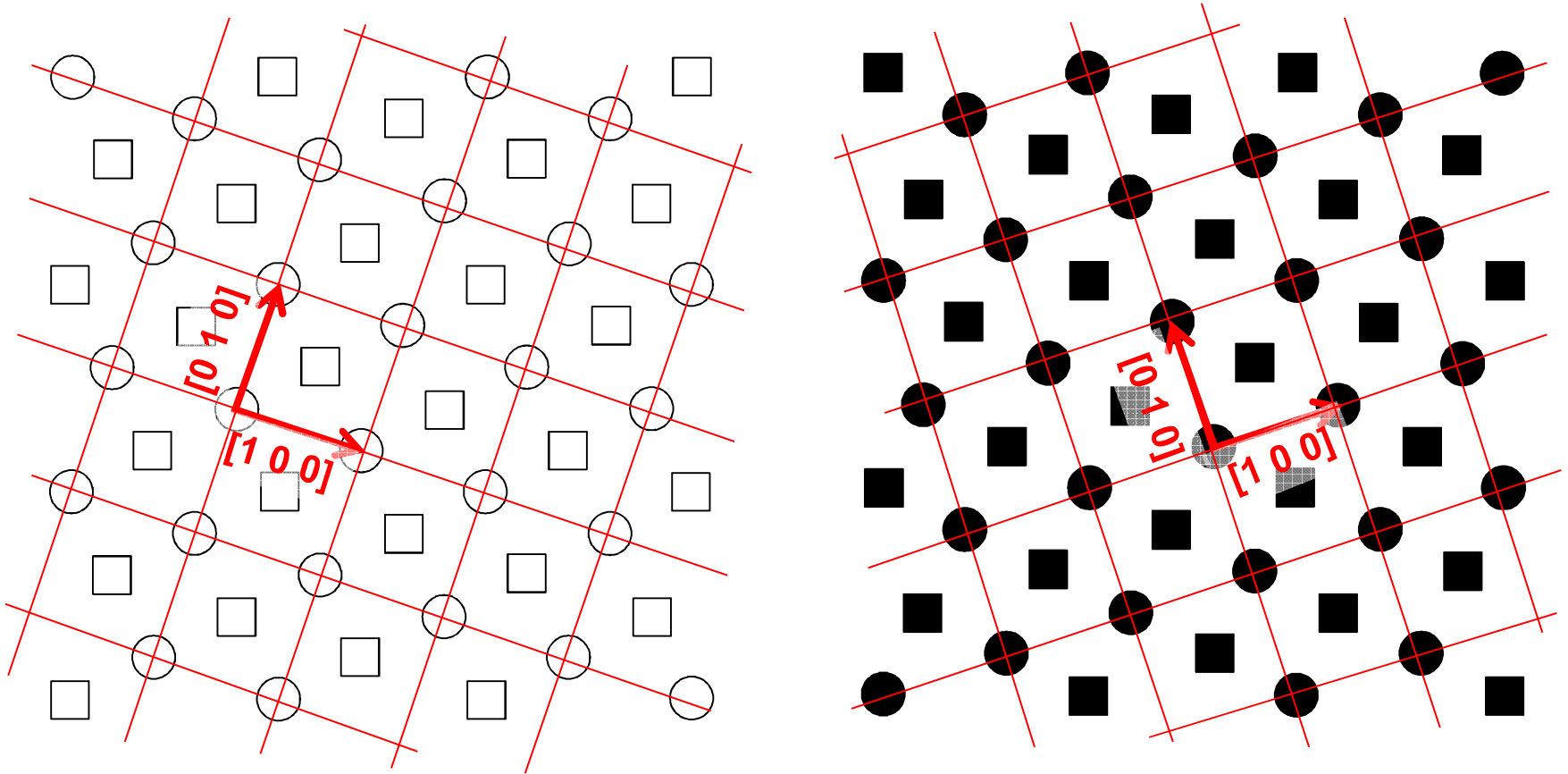
Observations: Polycrystalline BCC Fe film



Measured misorientation: $34.49^\circ \pm 0.7^\circ$
Very close to $\Sigma=5$: $\theta_{\Sigma=5}=36.87^\circ$
 $\Delta\theta = -2.38^\circ$

Pulsed Laser Deposited Fe on Rocksalt (NaCl). 36 nm thickness.
Specimen released and annealed on Mo grid 675°C, 2 hours.
under vacuum

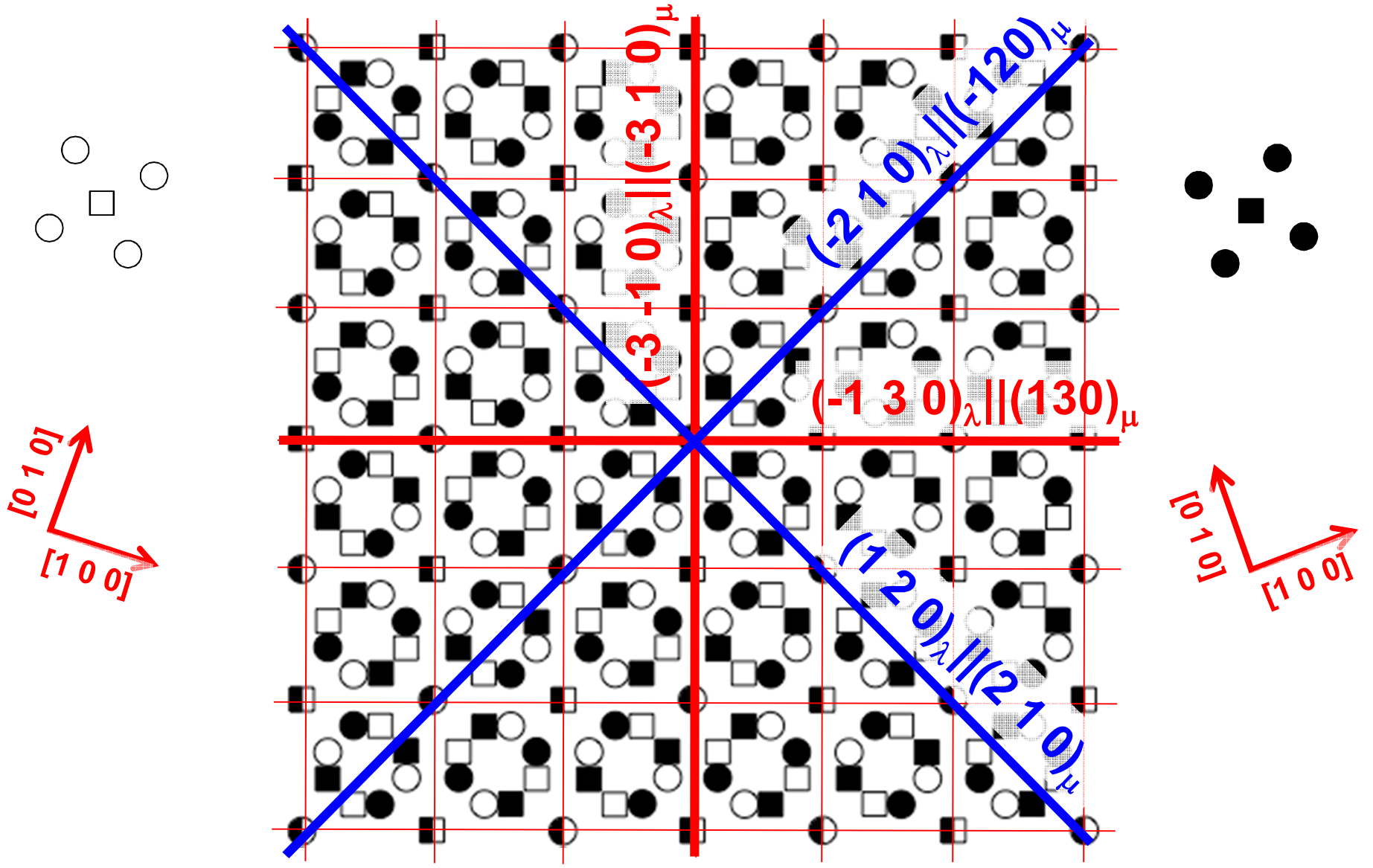
BCC $\Sigma=5$ [001]: Interfacial Crystallography



36.87° Rotation about [001]

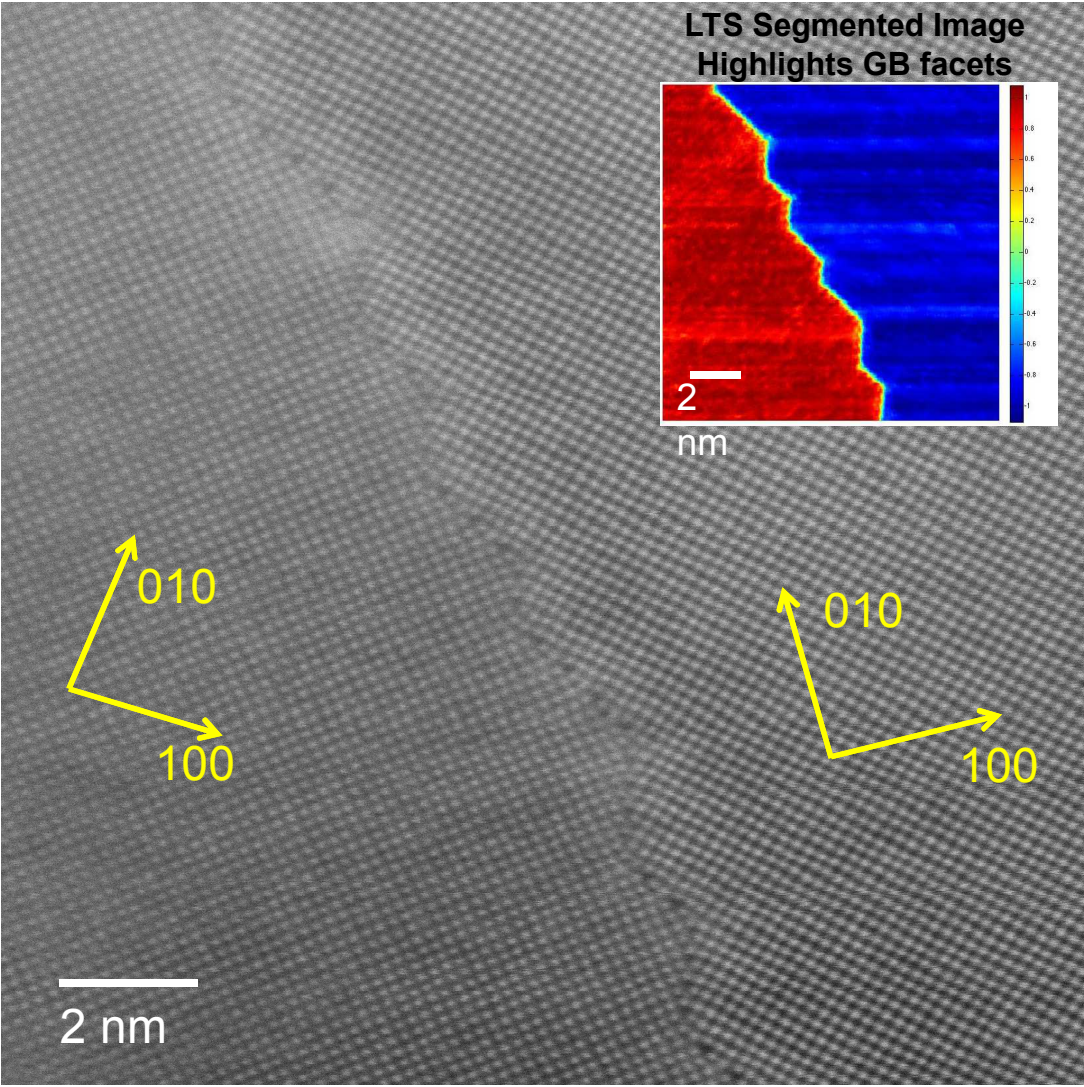
BCC $\Sigma=5$ [001]: Interfacial Crystallography

Dichromatic Pattern

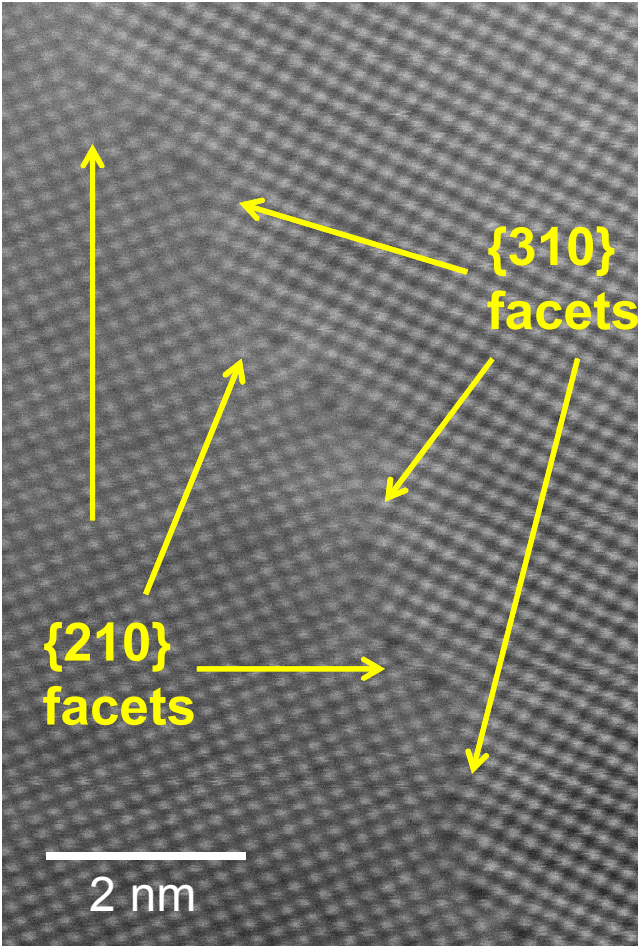


HRSTEM shows nanoscale faceting at Grain boundary Sandia National Laboratories

HAADF-STEM $\Sigma=5$ $\langle 001 \rangle$ Boundary in Fe

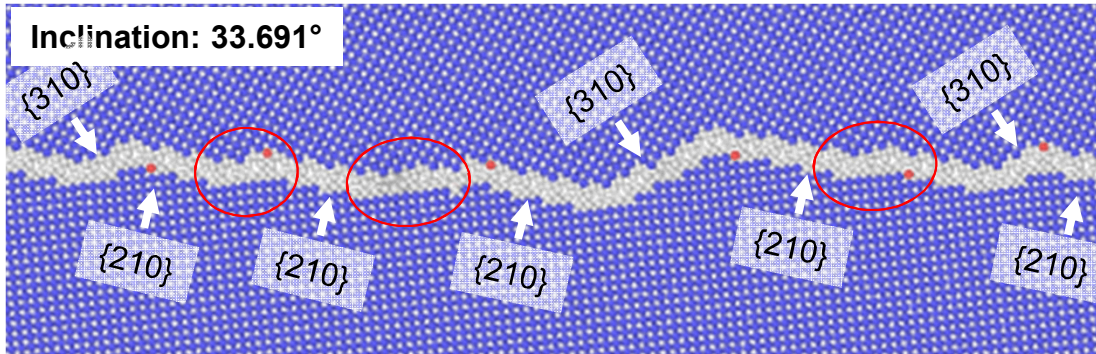
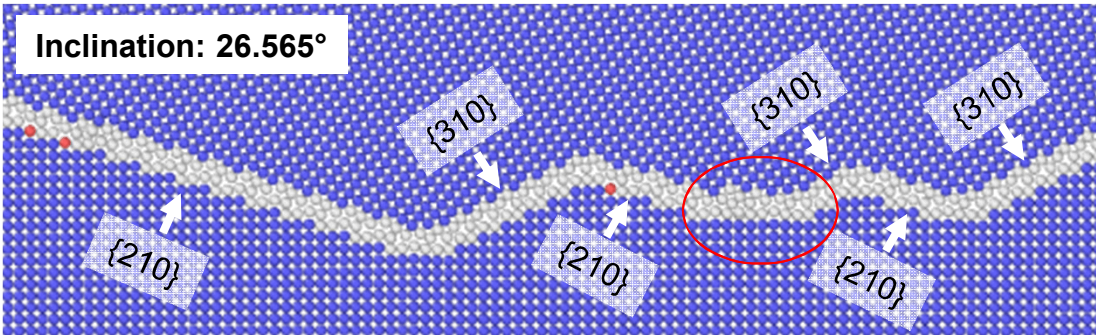
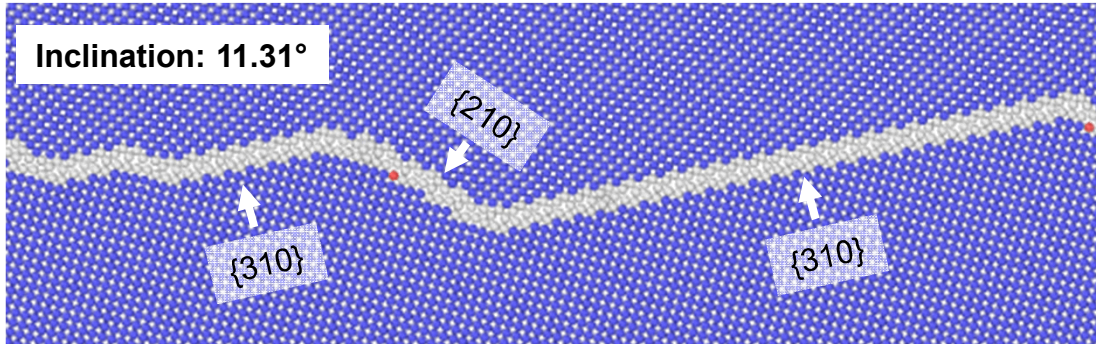


Boundary is faceted on $\{210\}$ and $\{310\}$ type inclinations



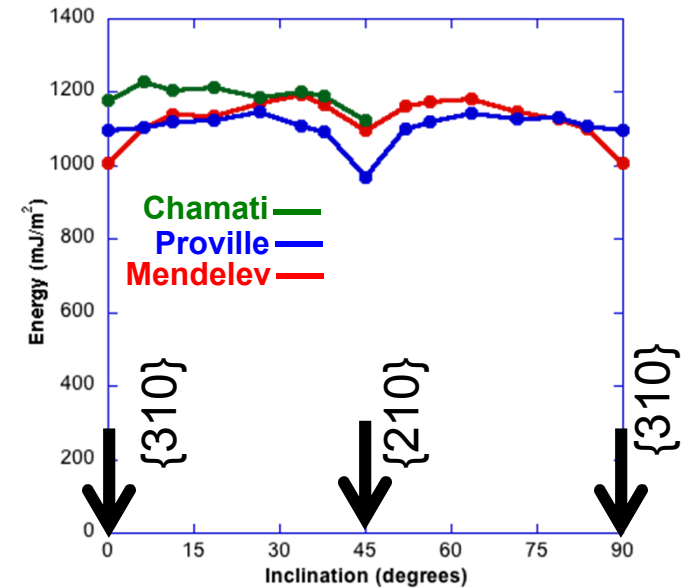
Inclination from $\{310\}$: $\approx 25^\circ$

Variation in Structure and Energy with inclination: MD shows 310 and 210 faceting



Mendelev Potential

GB Energy vs. Inclination



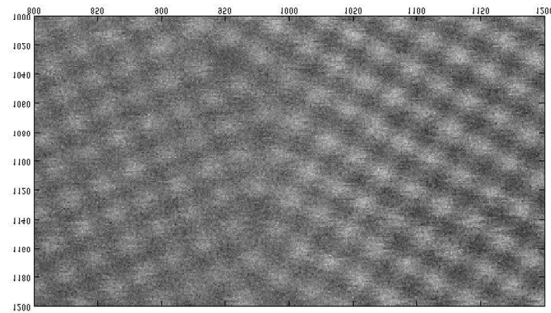
Atomistics show dissociation into coexisting {310} and {210} facets.

Additional faceting on {710}/{110} planes:

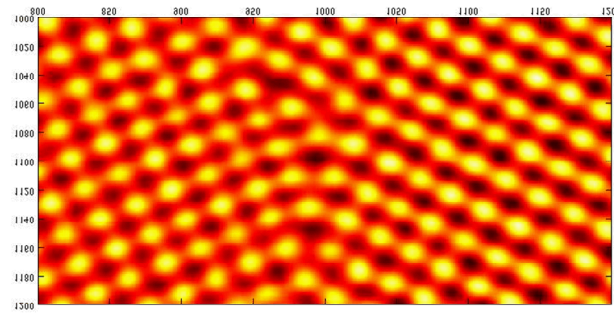
- 1:1 ratio of {310} and {210} units
- Not fully coarsened into lower energy {210}, {310} facets.

Quantifying the GB Images: Peak Location

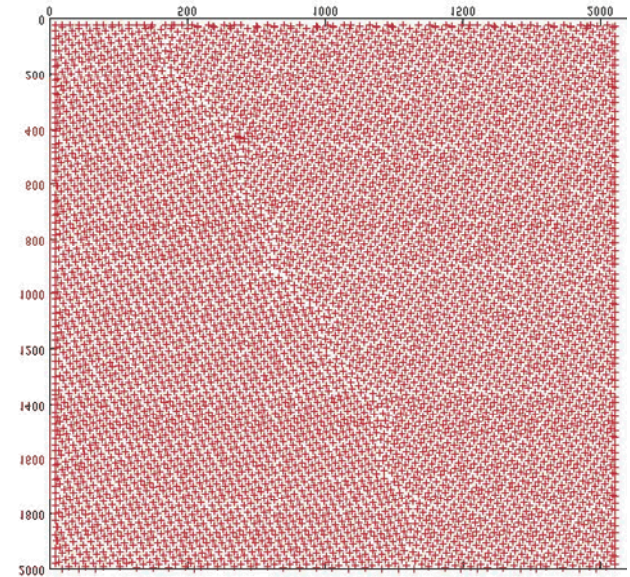
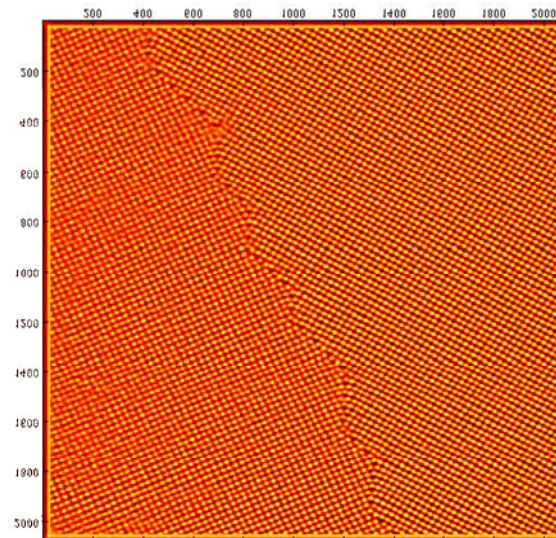
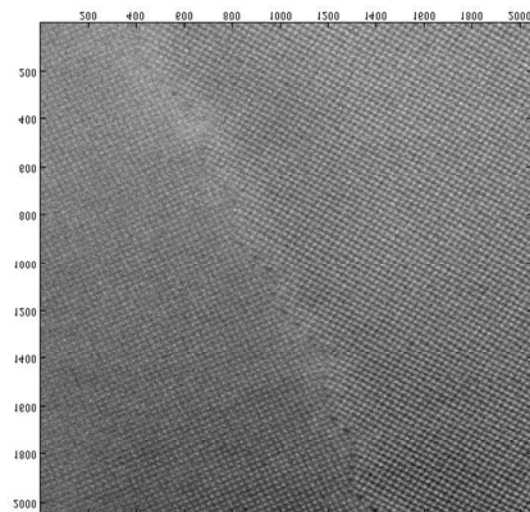
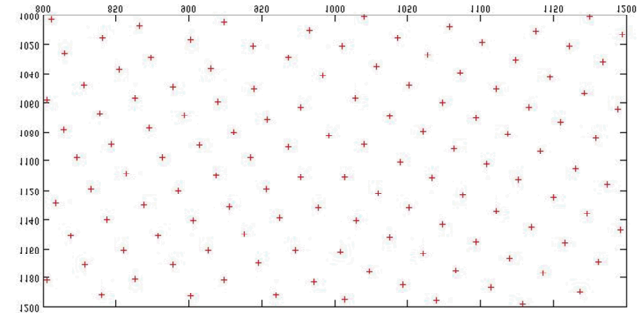
Raw HAADF STEM Image



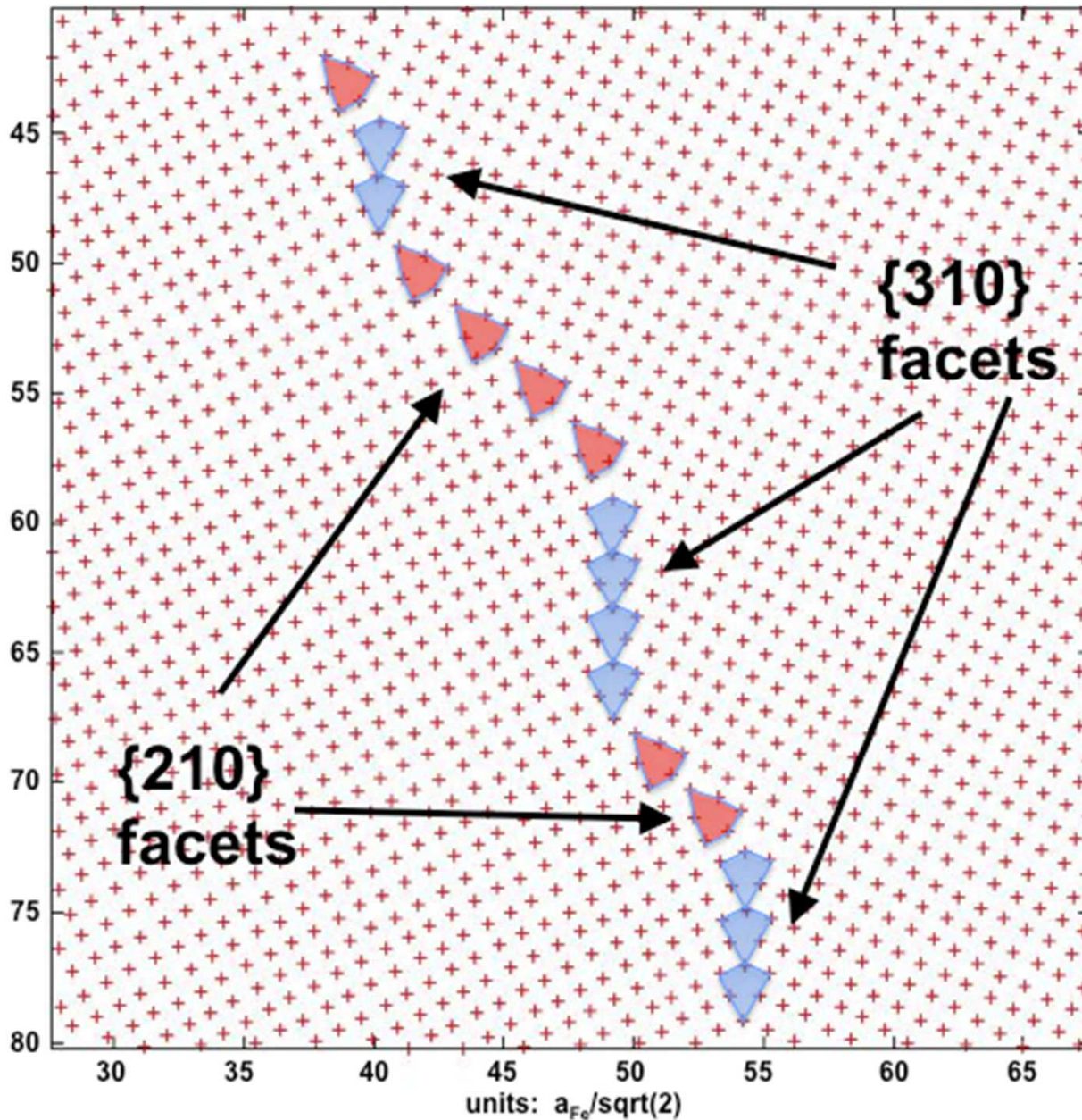
Correlation Image-Gaussian



Peak Positions



**Shear distortion due to specimen drift during image acquisition.
Corrected by affine transformation to peak position array.**

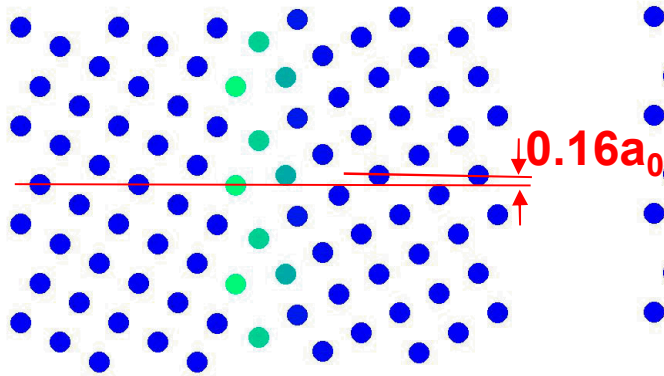


Intensity peak positions from HAADF-STEM of Fe $\Sigma=5$ grain boundary

How do the {310} and {210} structural units compare with atomistic predictions?

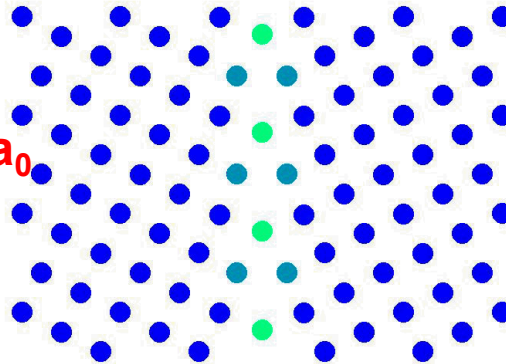
$\Sigma=5$ {310} Structures with different Potentials

Asymmetric



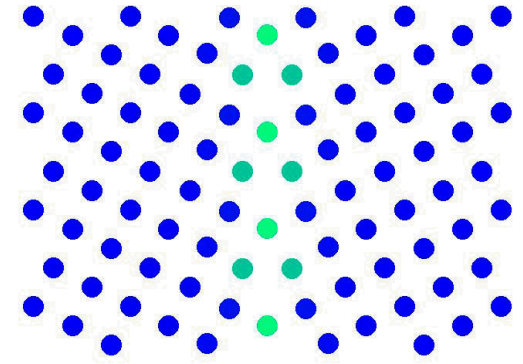
Potential: Chamati, 2006

Symmetric



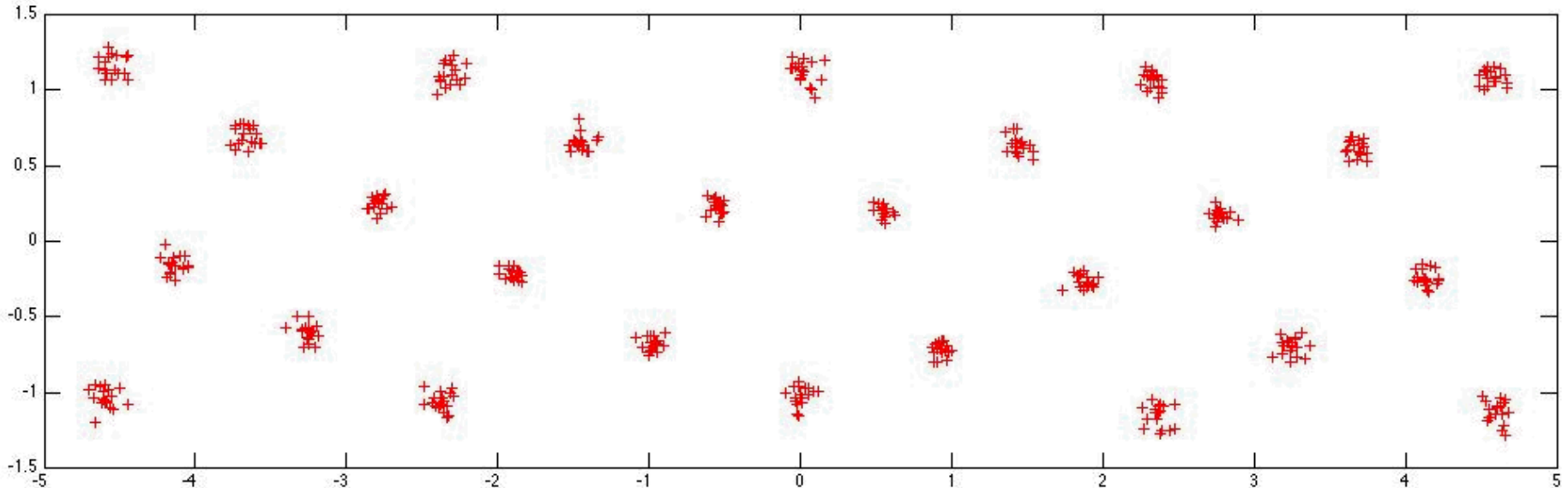
Potential: Mendeleev, 2003

Symmetric



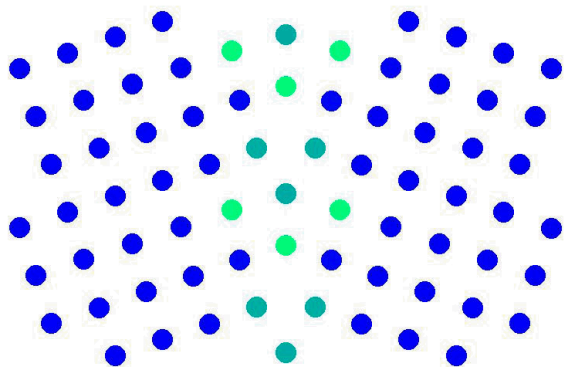
Potential: Proville, 2012

Experimental Peak Positions (HAADF STEM) $\Delta y = -0.015 \pm 0.036 a_0$



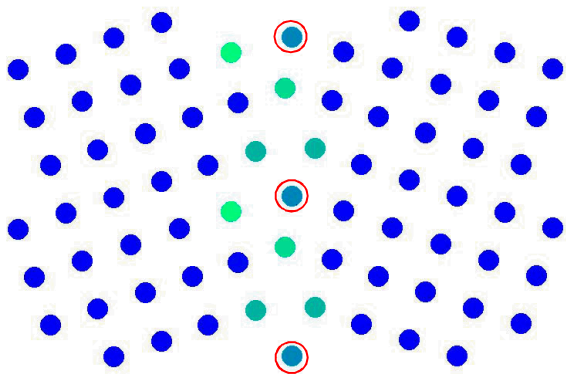
$\Sigma=5$ {210} Structures with different Potentials

Symmetric



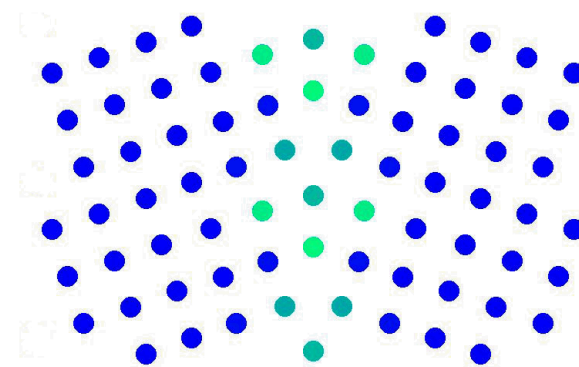
Potential: Chamati, 2006

Asymmetric



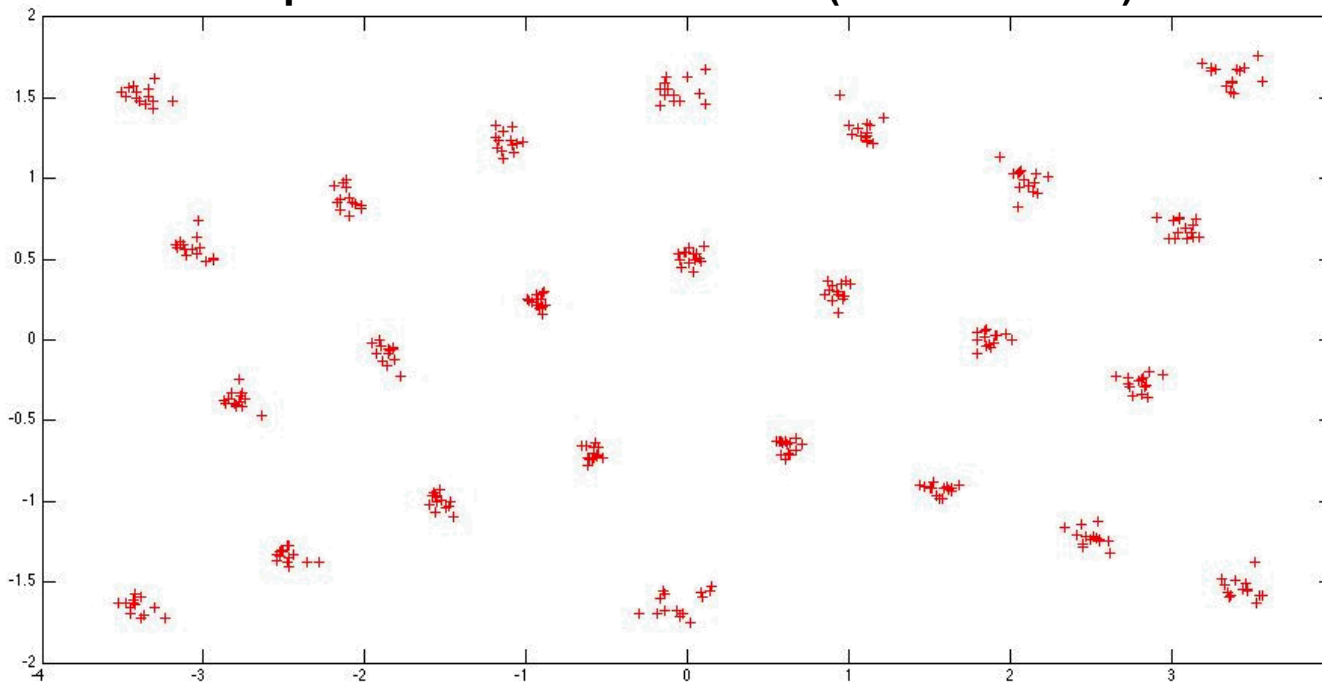
Potential: Mendeleev, 2003

Symmetric



Potential: Proville, 2012

Experimental Peak Positions (HAADF STEM)



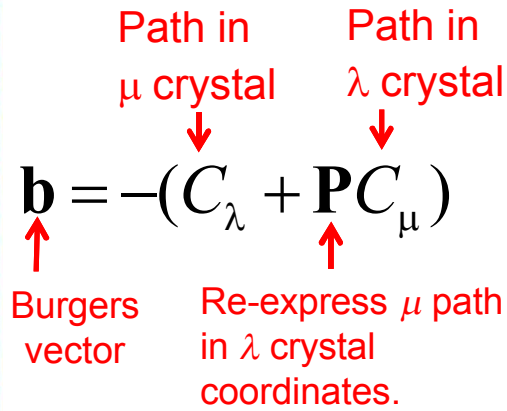
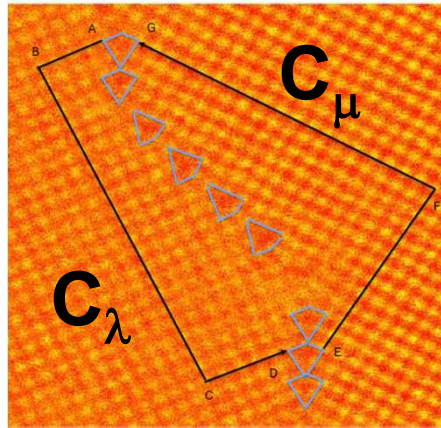
$$\Delta y = 0.035 \pm 0.015 a_0$$

Are Grain Boundary Dislocations Present?

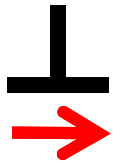
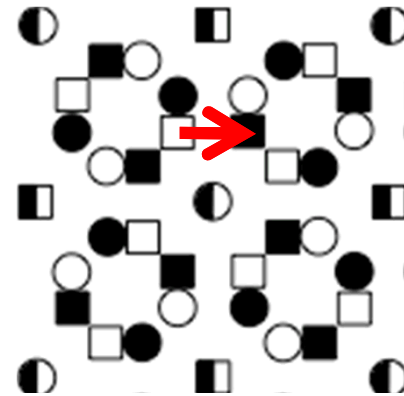
Boundary is misoriented from exact $\Sigma=5$ ($\Delta\theta=-2.38^\circ$)

Determine defect content by Circuit Mapping over all facet junctions

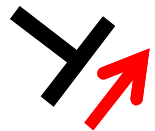
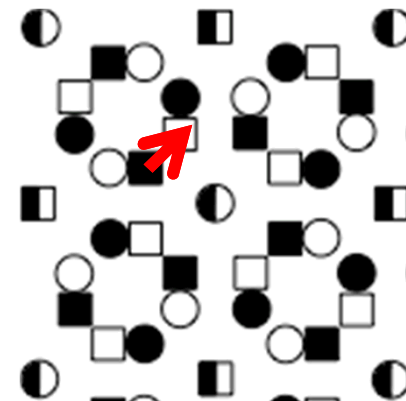
Two types of defect observed:



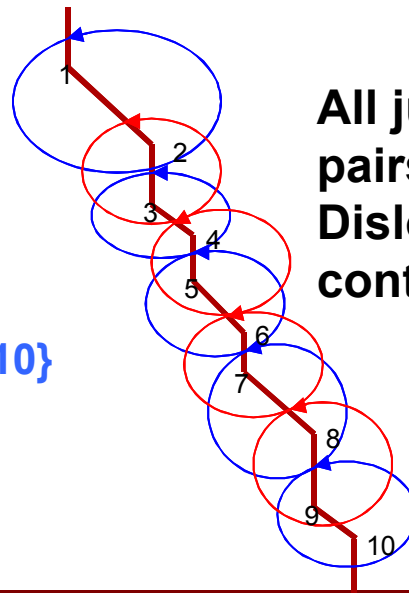
$\mathbf{b} = (1/5)[3, 1, 0]$



$\mathbf{b} = (1/5)[1, 2, 0]$

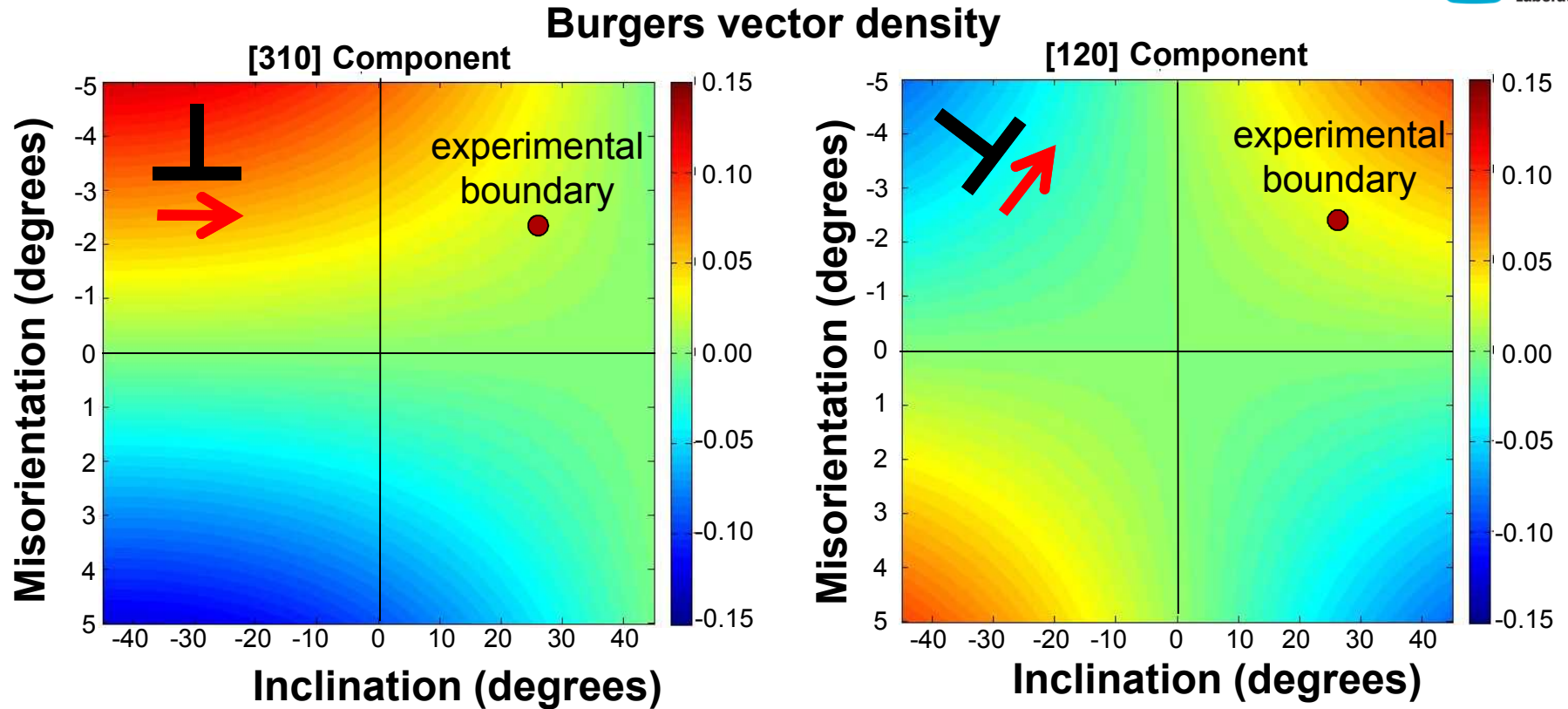


- Circuits must cross at equivalent GB sites
- Every circuit then includes 2 junctions.
- Alternate between circuits on $\{210\}$ and $\{310\}$ inclinations



All junction pairs exhibited Dislocation content

Defect content tied to misorientation and inclination



- Burgers vector density related to misorientation and inclination through Frank-Bilby Equation: $B=(I-P^{-1}) v$

Experimental

<310> component: 0.0323

<120> component: 0.0152

Frank-Bilby equation ($\theta=-2.38^{\circ}\pm 0.8^{\circ}, \phi=25.9\pm 1.0^{\circ}$)

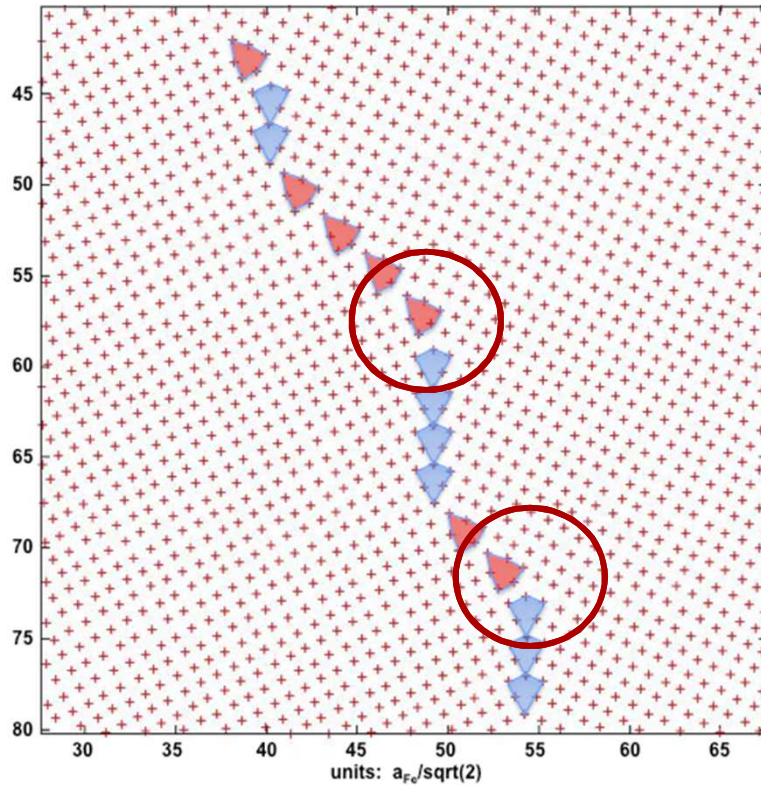
<310> component: 0.0180 ± 0.006

<120> component: 0.027 ± 0.010

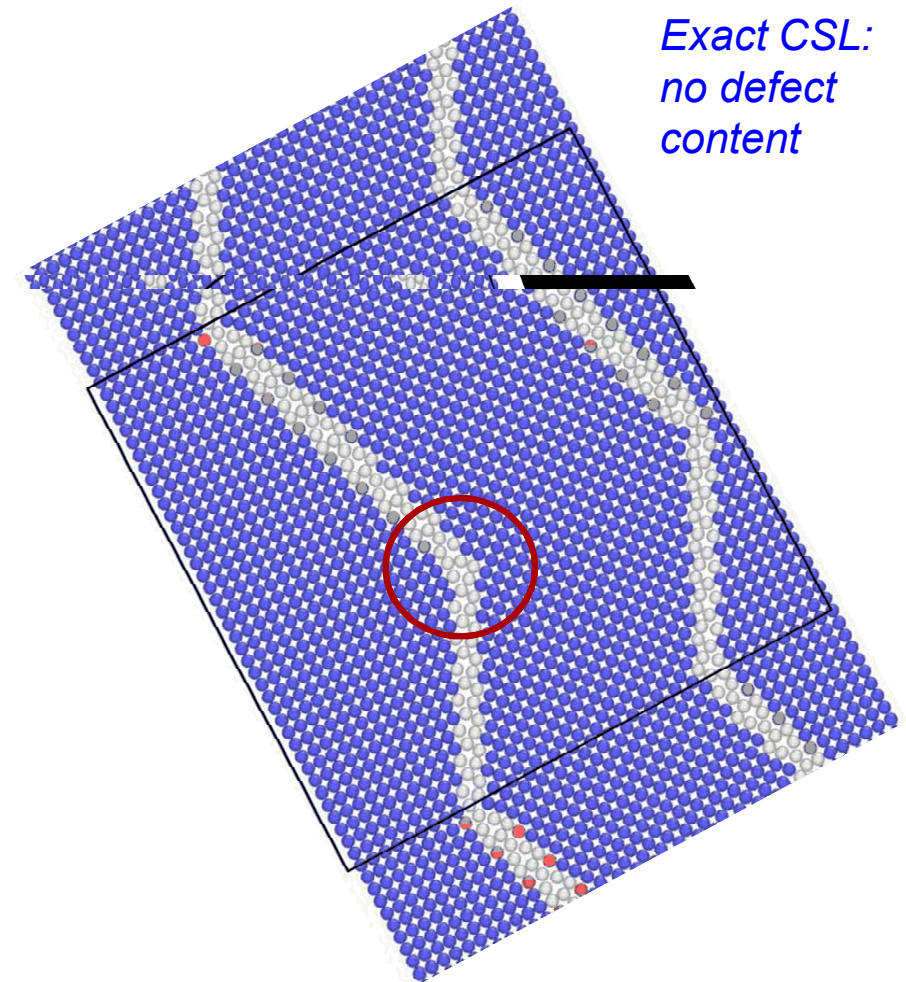
- For inclinations away from {310}, b_{120} component required to accommodate interfacial coherency strains.

How are the grain boundary dislocations manifested in the junction structure?

Experimental Junctions
 $b=(1/5)(120)$ and $(1/5)(310)$



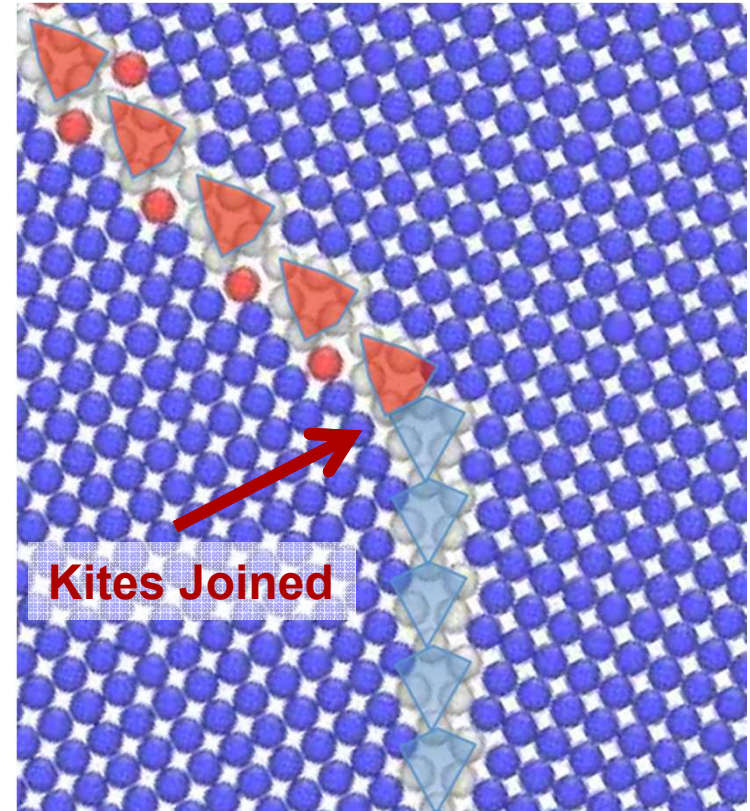
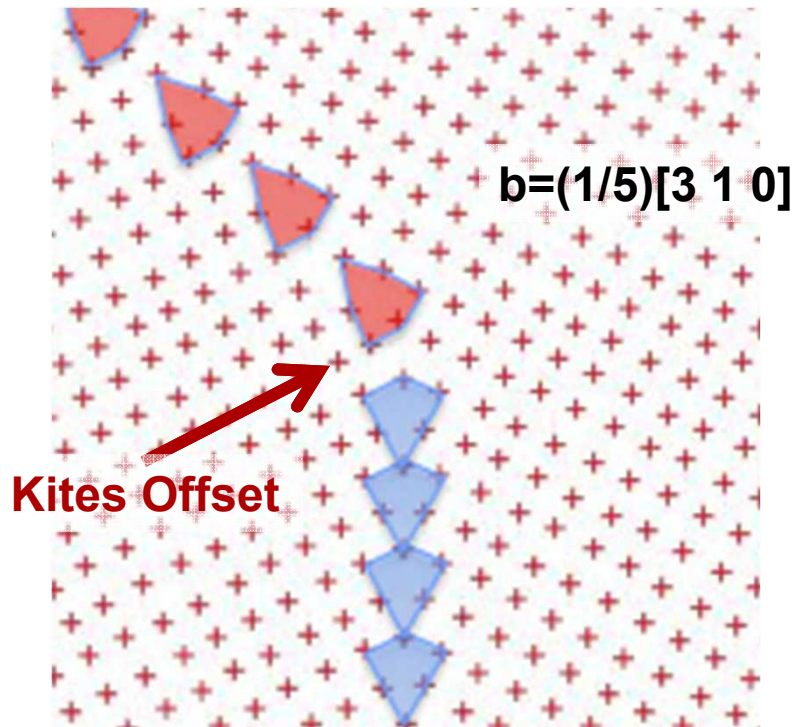
Relaxed Periodic Atomistic Structure



How are the grain boundary dislocations manifested in the junction structure?

Experimental Junctions
 $b=(1/5)(120)$ and $(1/5)(310)$

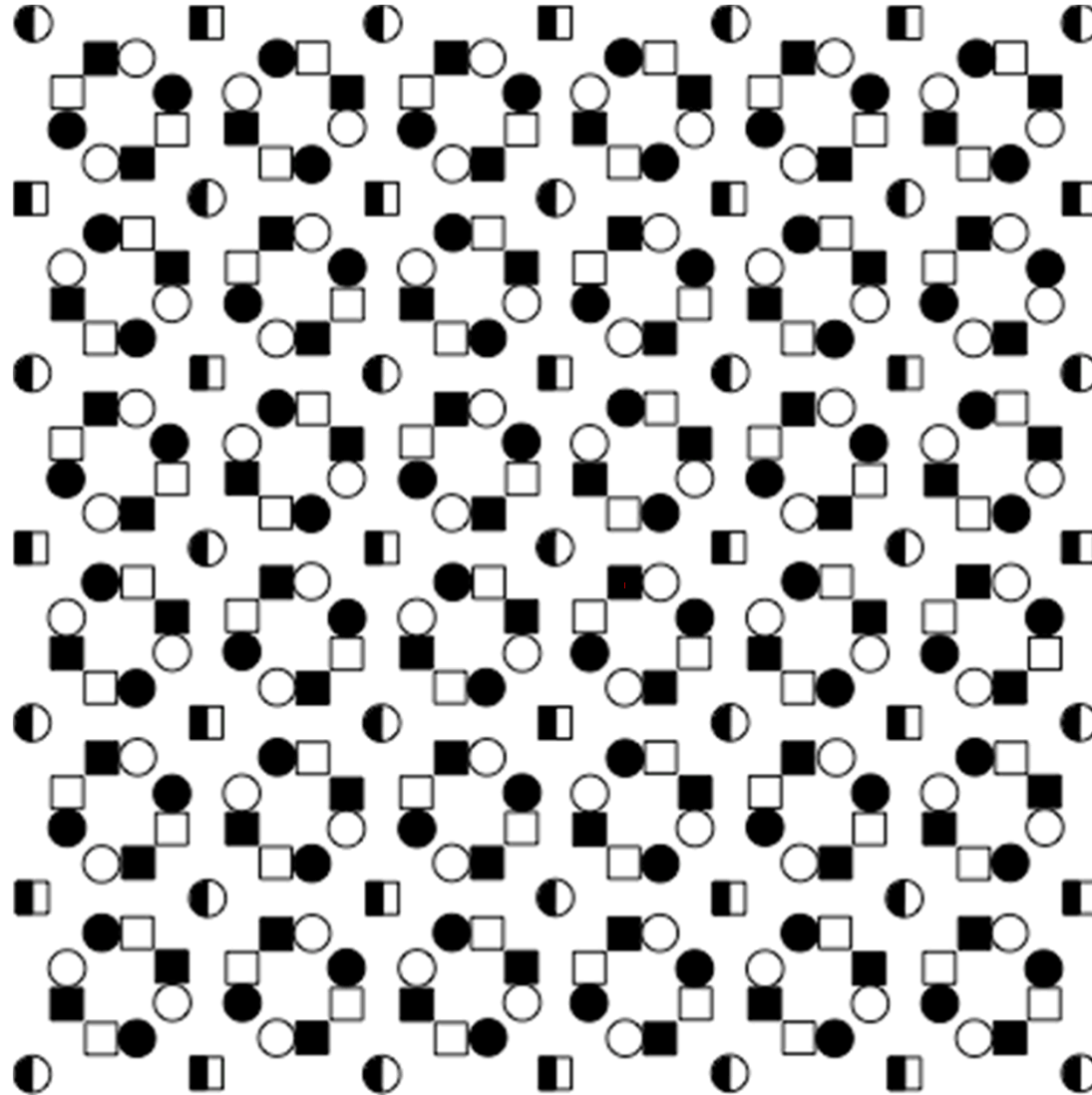
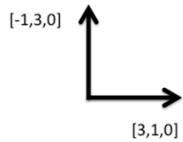
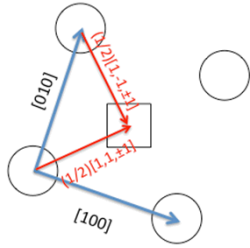
Relaxed Periodic Atomistic Structure



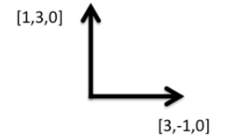
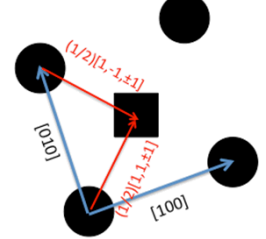
Geometric origin of the junction structure

$\Sigma=5$
Dichromatic
Pattern

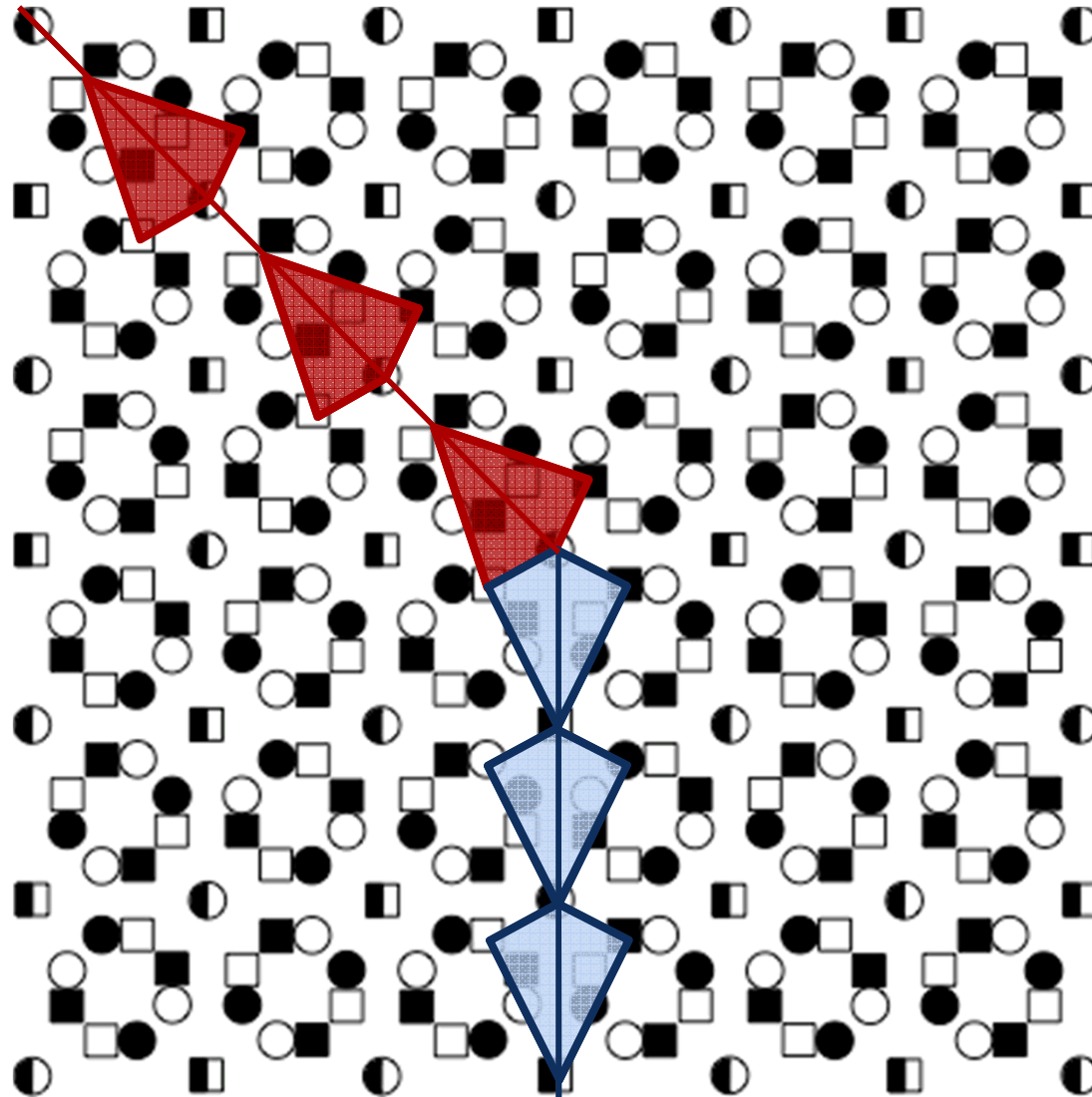
λ =white



μ =black

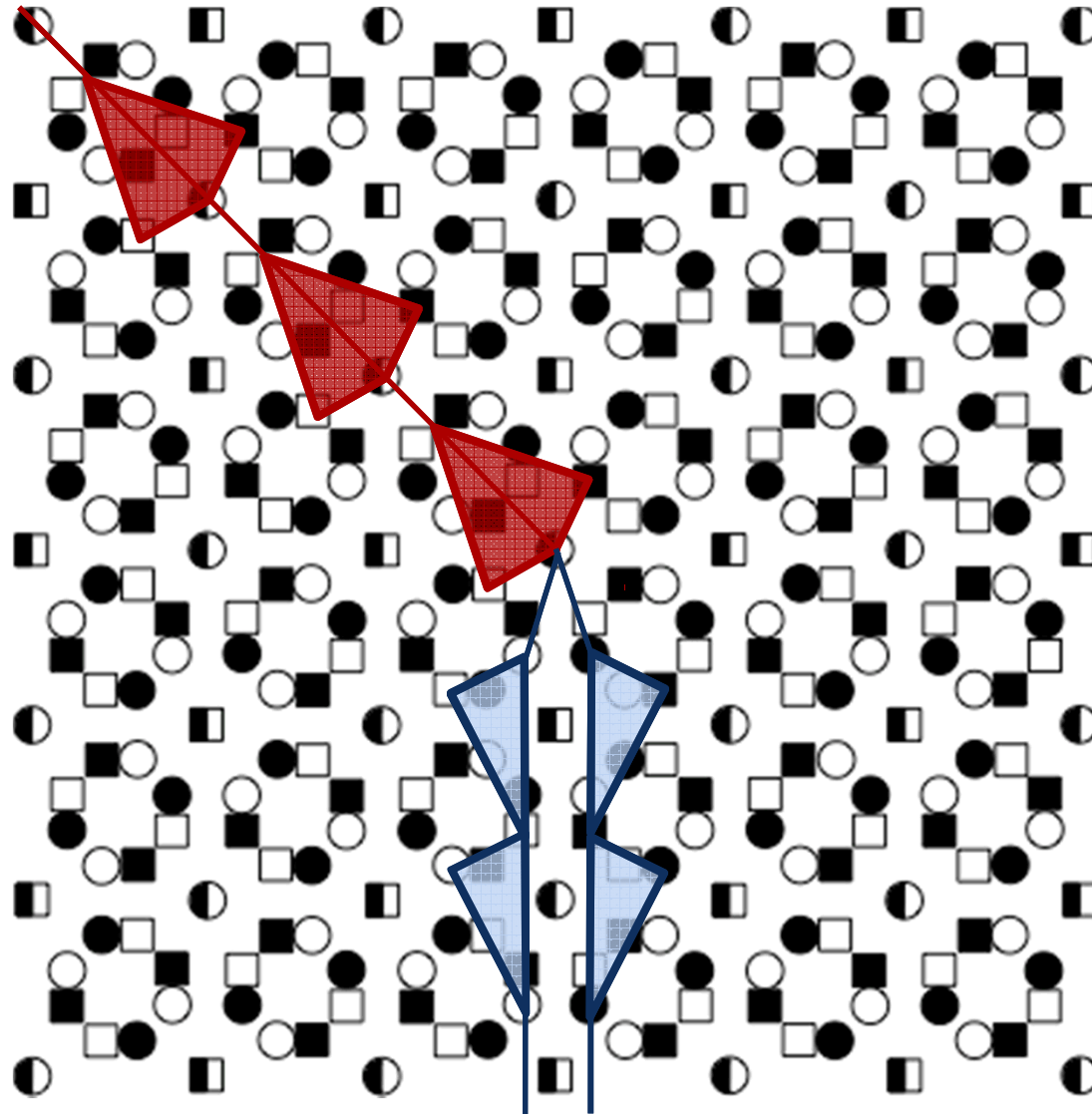


Geometric origin of the junction structure



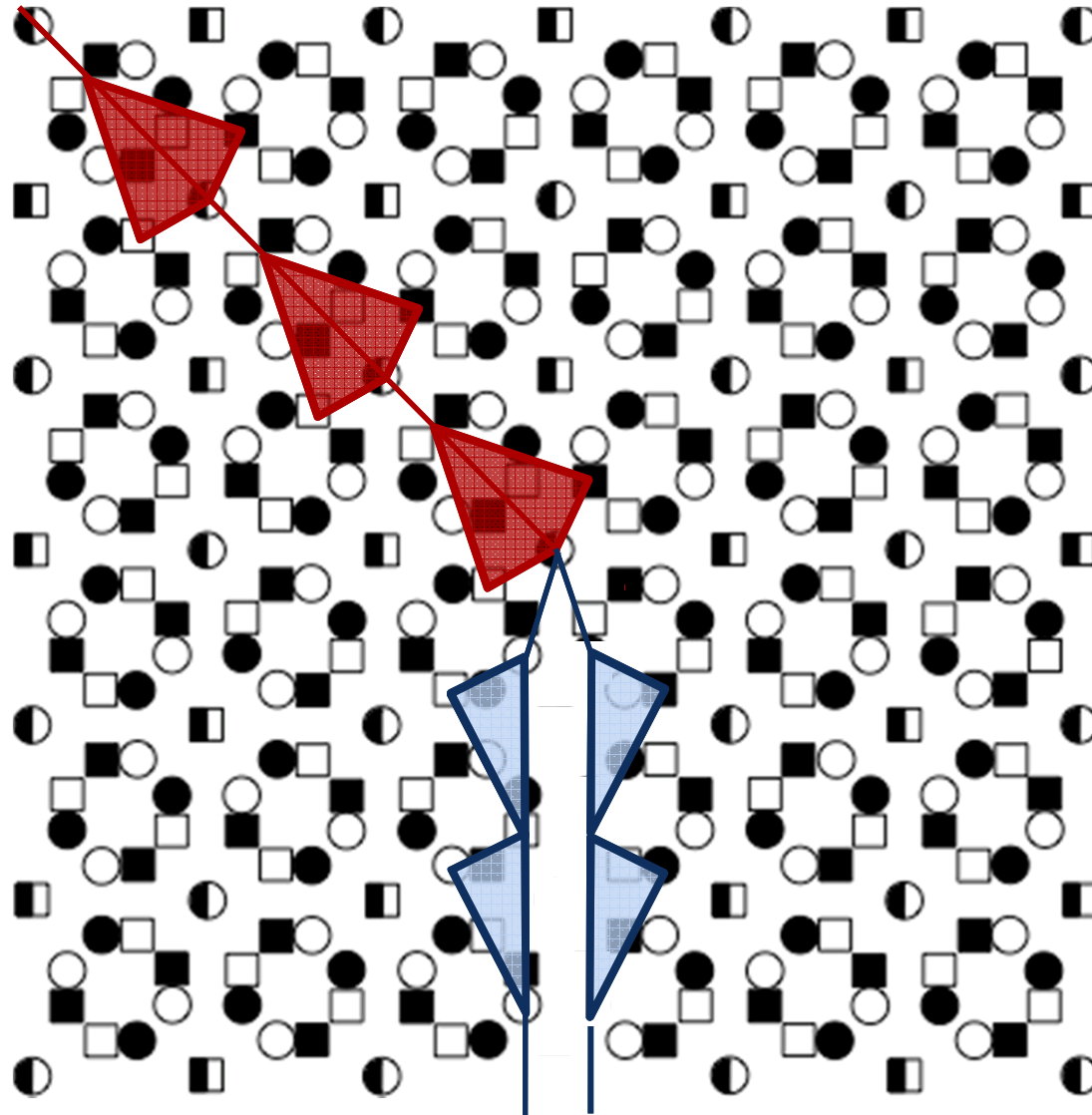
Geometric origin of the junction structure

Remove
material from
half-plane
of width
 $(1/5)[310]$

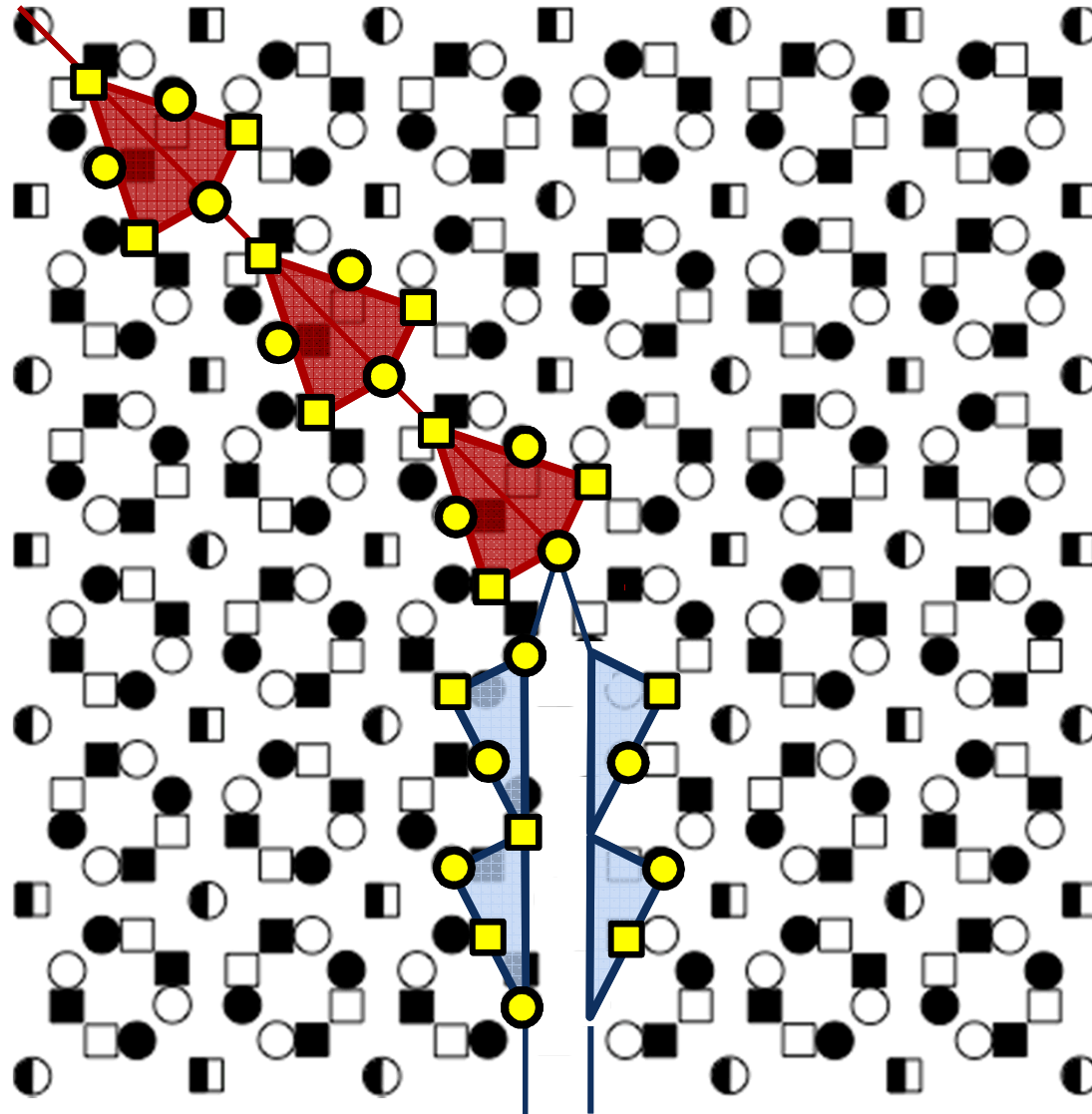


Geometric origin of the junction structure

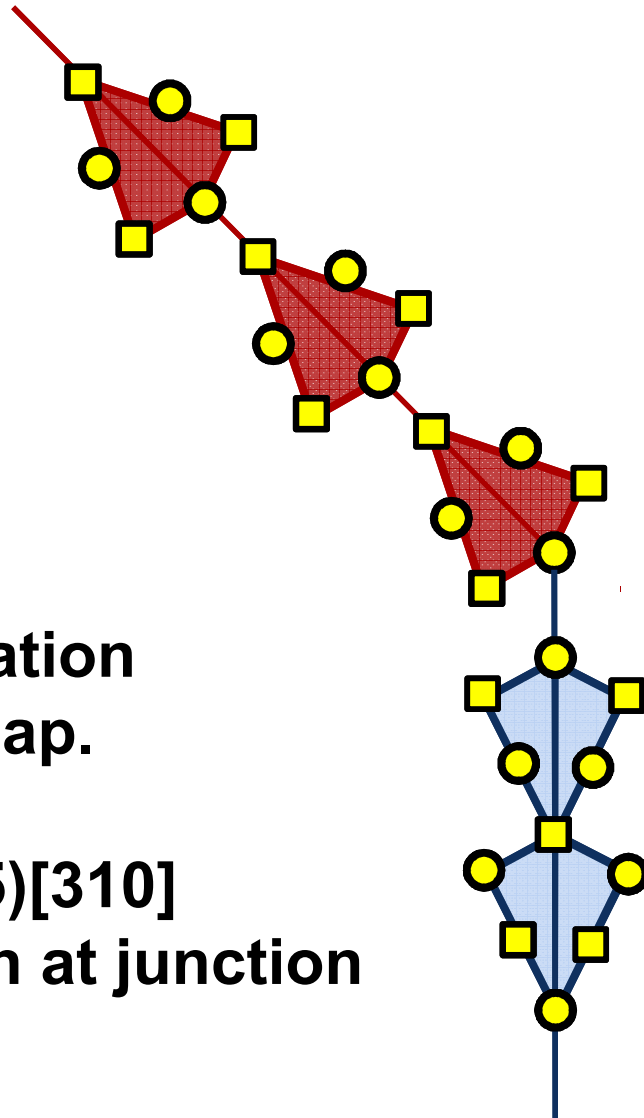
Remove
material from
half-plane
of width
 $(1/5)[310]$



Geometric origin of the junction structure



Geometric origin of the junction structure



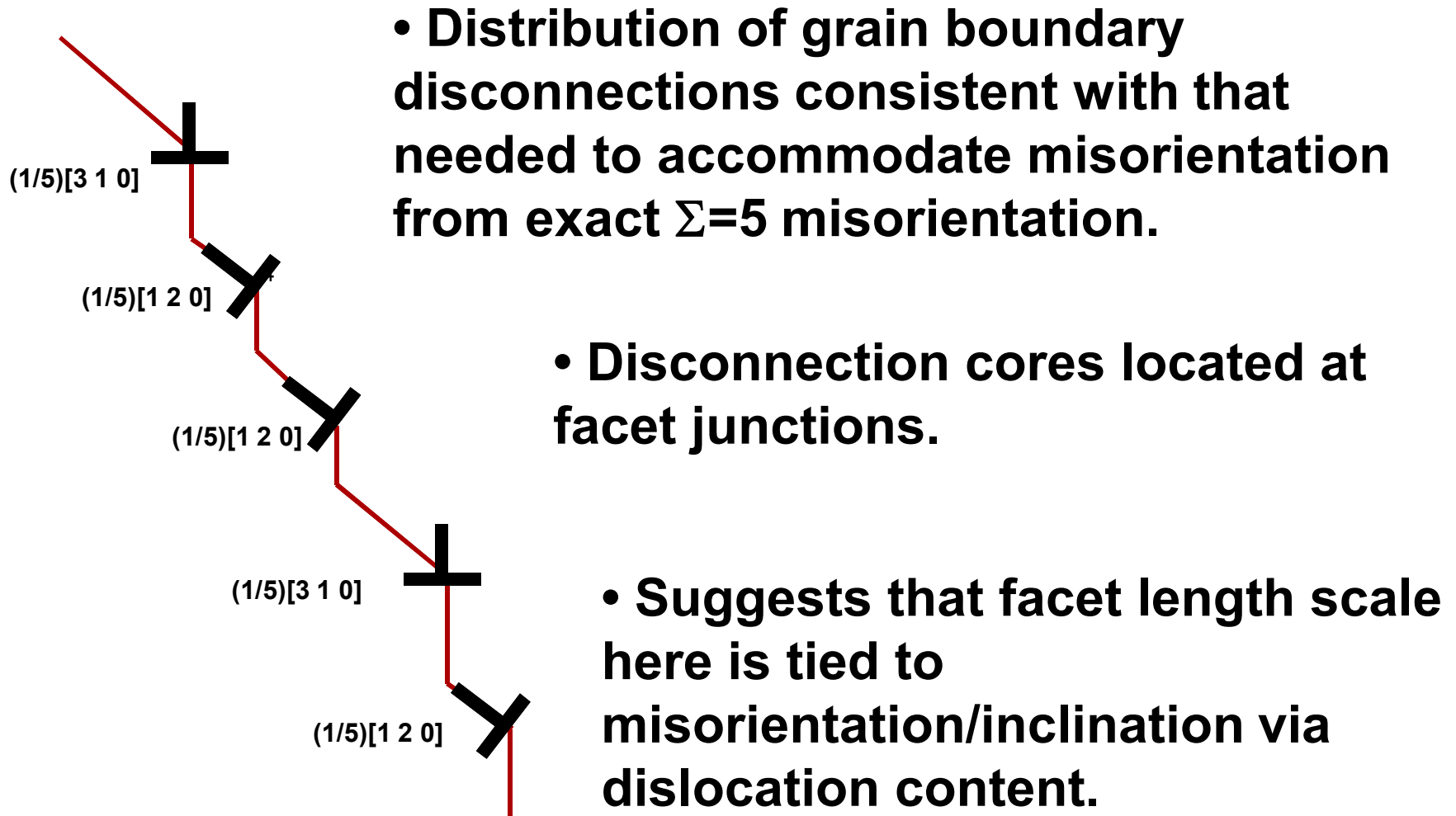
Kites are now off-set

**Volterra operation
to close the gap.**

**Creates a $(1/5)[310]$
disconnection at junction**

**Similar
construction for
 $(1/5)[120]$
disconnection**

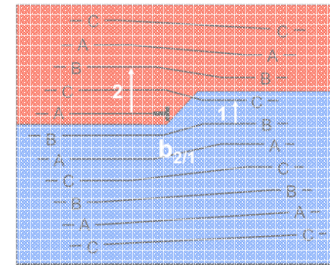
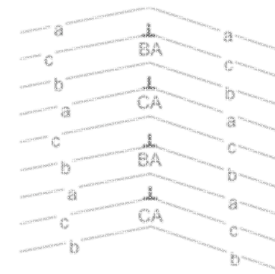
Impact on facet length scale



Outline

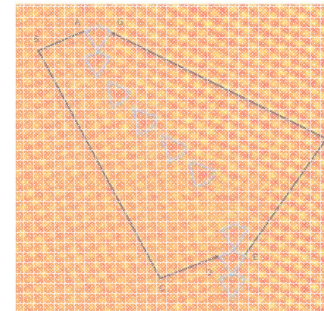
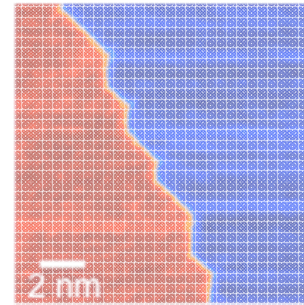
Background on Interfacial Line defects

- Overview of defect types
- Examples from low and high angle GBs.



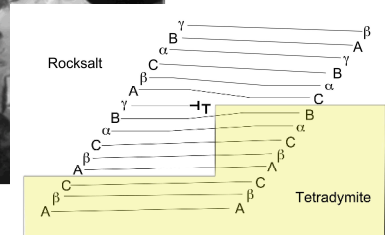
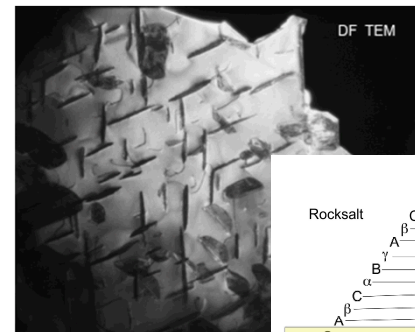
GB disconnections and facet junctions

- Asymmetric $\Sigma=5$ GB in BCC Fe
- Interplay of facet junctions and grain boundary disconnections

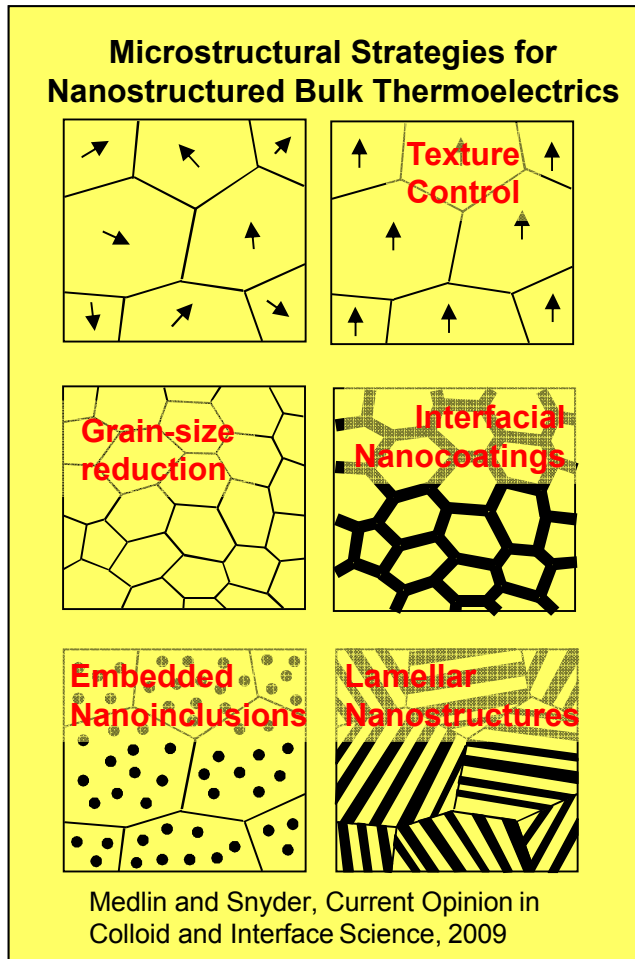


Disconnections at heterophase interfaces

- Telluride precipitates in thermoelectric alloy.
- Role of disconnections in transformation mechanism and interfacial strain relief.



Bulk Thermoelectrics: Control of Microstructure to Improve Performance



TE Energy Conversion Efficiency: Figure of Merit

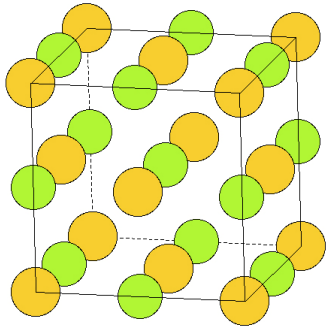
$$zT = \frac{S^2 \sigma}{\kappa} T$$

Seebeck Coefficient S
 Electrical Conductivity σ
 Thermal Conductivity κ

- Variety of microstructural strategies for bulk thermoelectrics employ embedded interfaces to decouple thermal and electronic transport
- What are the atomic mechanisms that govern interface formation and stability?

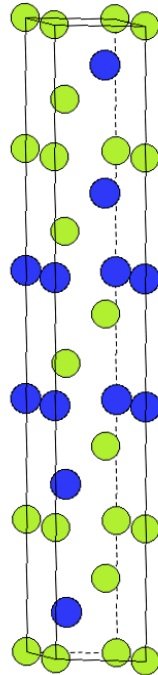
Heterophase Rocksalt/Tetradymite Telluride Interfaces

Rock-Salt
(PbTe, AgSbTe₂)



Fm-3m

Tetradymite
(Bi₂Te₃, Sb₂Te₃)



R-3m

What happens at interface?
How do transformations occur?
Misfit accommodation?

-Interest in forming thermoelectric nanocomposites of rock-salt and tetradymite tellurides:

- Possibility for well ordered interfaces.
- Transformations provide bulk route to synthesis.

Ikeda, et al., Chem Mater. 2007

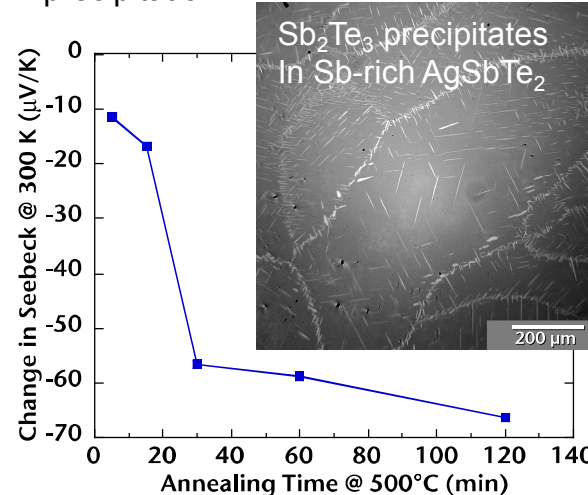
Snyder and Toberer, Nature Materials 2008

-AgSbTe₂:

- Constituent of TAGS (GeTe)_x(AgSbTe₂)_{1-x} and LAST (PbTe)_x(AgSbTe₂)_{1-x} zT ~ 1.8

- High performance TE material: zT > 1.2

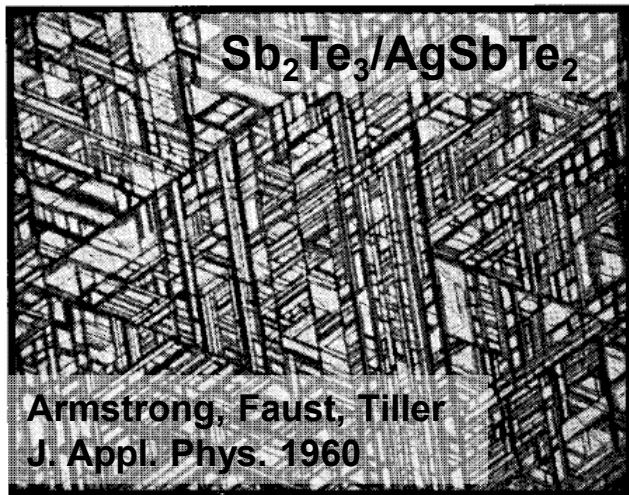
- Degradation of Seebeck coefficient with Sb₂Te₃ precipitation



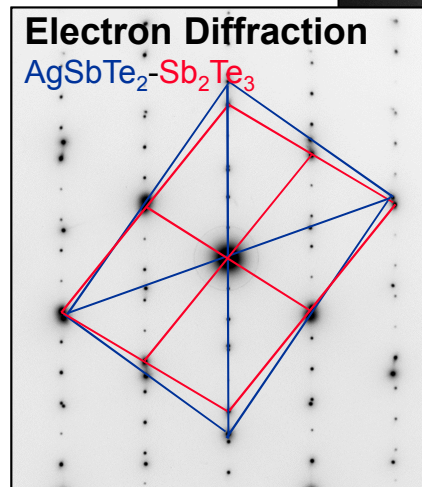
Sharma, Sugar, Medlin J. Appl. Phys. 2010

Crystallographic alignment between rocksalt and tetradymite phases

Widmanstätten plates

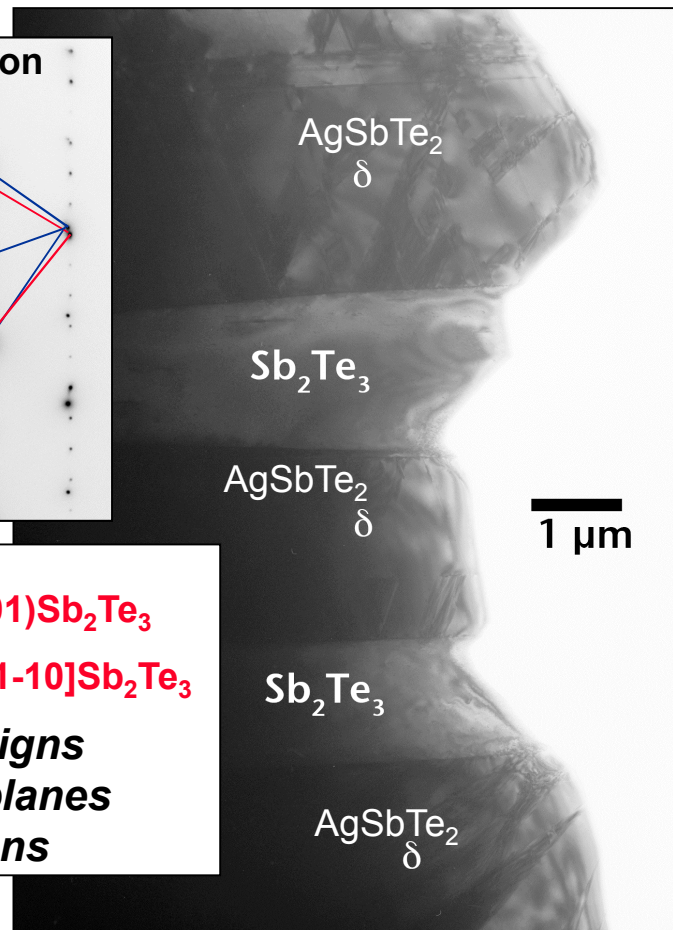


TEM $Sb_2Te_3/AgSbTe_2$



$(111)AgSbTe_2 // (0001)Sb_2Te_3$
 $[-101]AgSbTe_2 // [2-1-10]Sb_2Te_3$

*Orientation aligns
close-packed planes
and directions*



Medlin and Sugar,
Scripta Mat 2010

How to convert between the rocksalt and tetradymite structures?

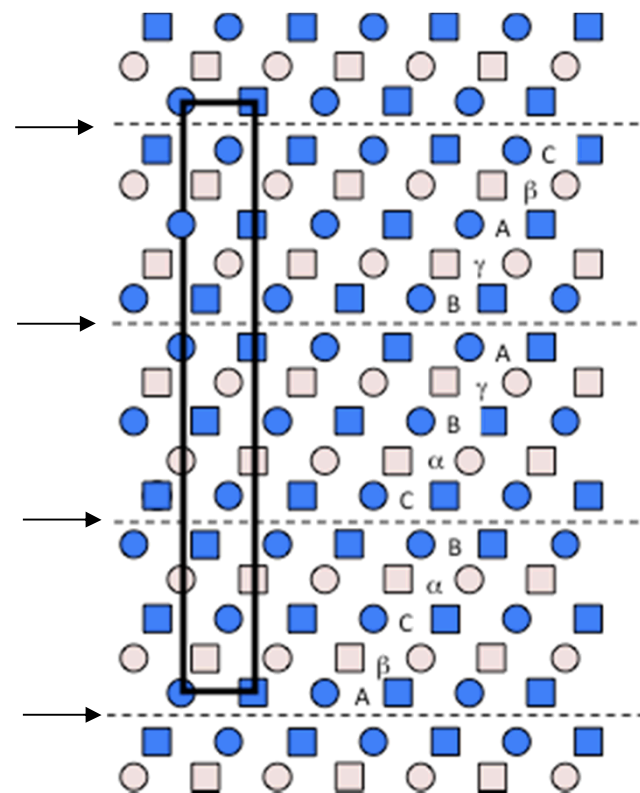
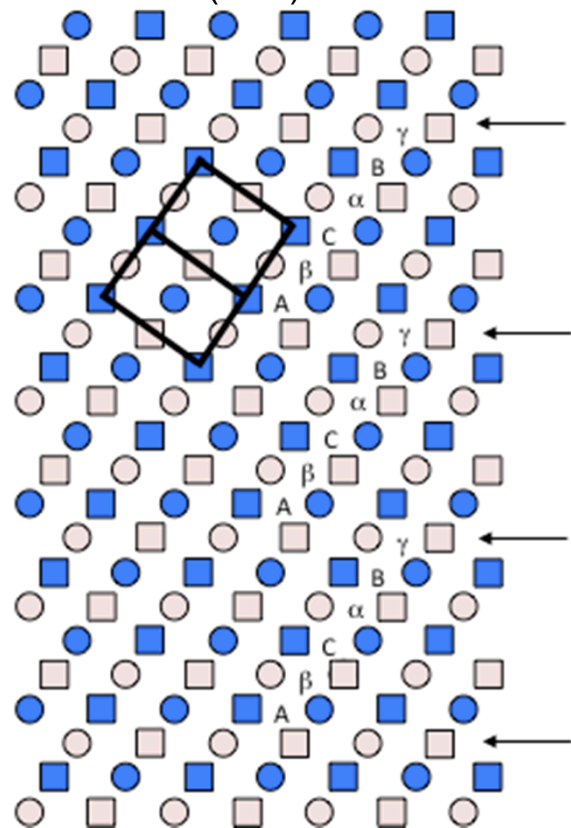
Rocksalt

Tetradymite

(MTe)

(M₂Te₃)

Te ●
Metal ○



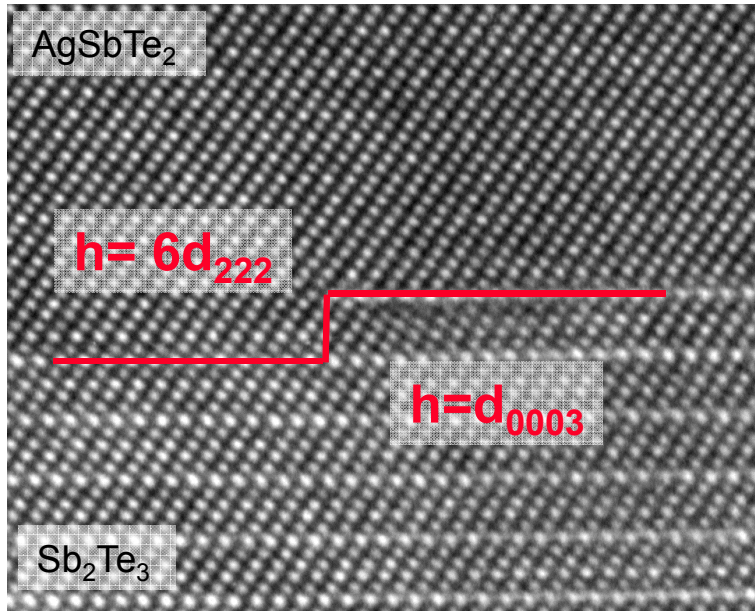
-Remove metal plane every 6 layers

-Shear blocks by $1/3\langle 10-10 \rangle$ (or $1/6\langle 112 \rangle$ relative to cubic coordinates)

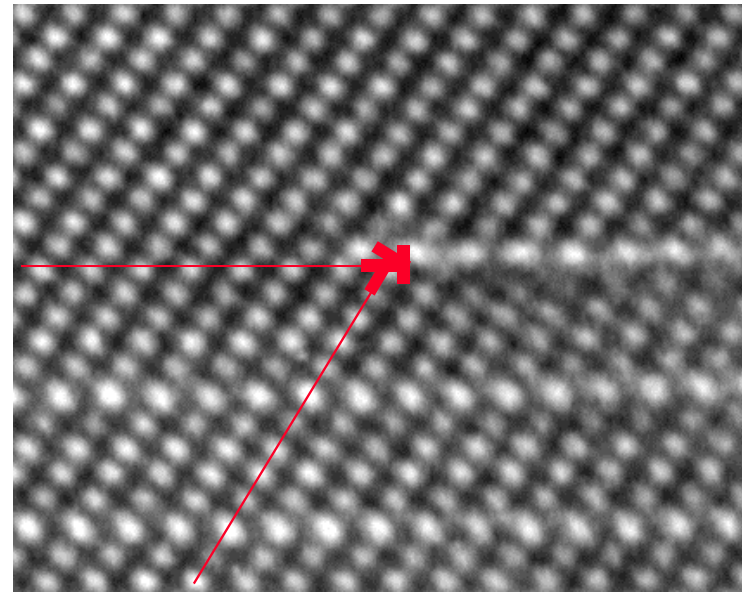
N. Frangis et al., J. Solid State Chemistry 84 (1990)

Transformation can be accomplished by motion of disconnections

HRTEM : Step at $\text{AgSbTe}_2/\text{Sb}_2\text{Te}_3$ Interface



JEOL 4000EX HRTEM



Defect has both *step* and *dislocation* character.

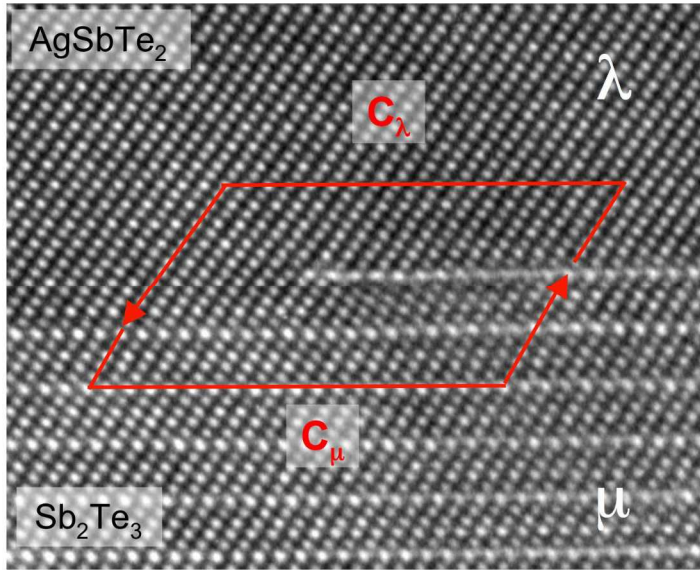
- Interfacial “Disconnection” (e.g. Hirth and Pond, Acta Mat 1996).
- Geometric properties of disconnections control mass flux and structural rearrangements of phase transformations.

Step joins *6 {222}* planes in AgSbTe_2 with *5 {000 15}* planes in Sb_2Te_3

Complex dislocation configuration.

Role of defect in precipitate growth:

Burgers vector:



Upper crystal circuit

Lower crystal circuit

$$\mathbf{b} = -(\mathbf{C}_\lambda + \mathbf{P}\mathbf{C}_\mu)$$

-Coordinate Transformation From Tetradyte to Rock-salt.
-Coherently strained reference frame

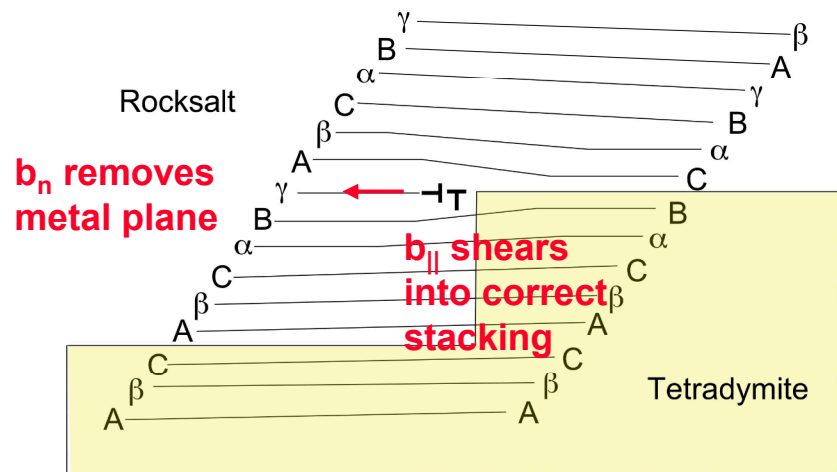
Resolve \mathbf{b} into components normal and parallel to interface

$$\mathbf{b}_n = (a_{cub} - c_{hex} / 3\sqrt{3})[111]$$

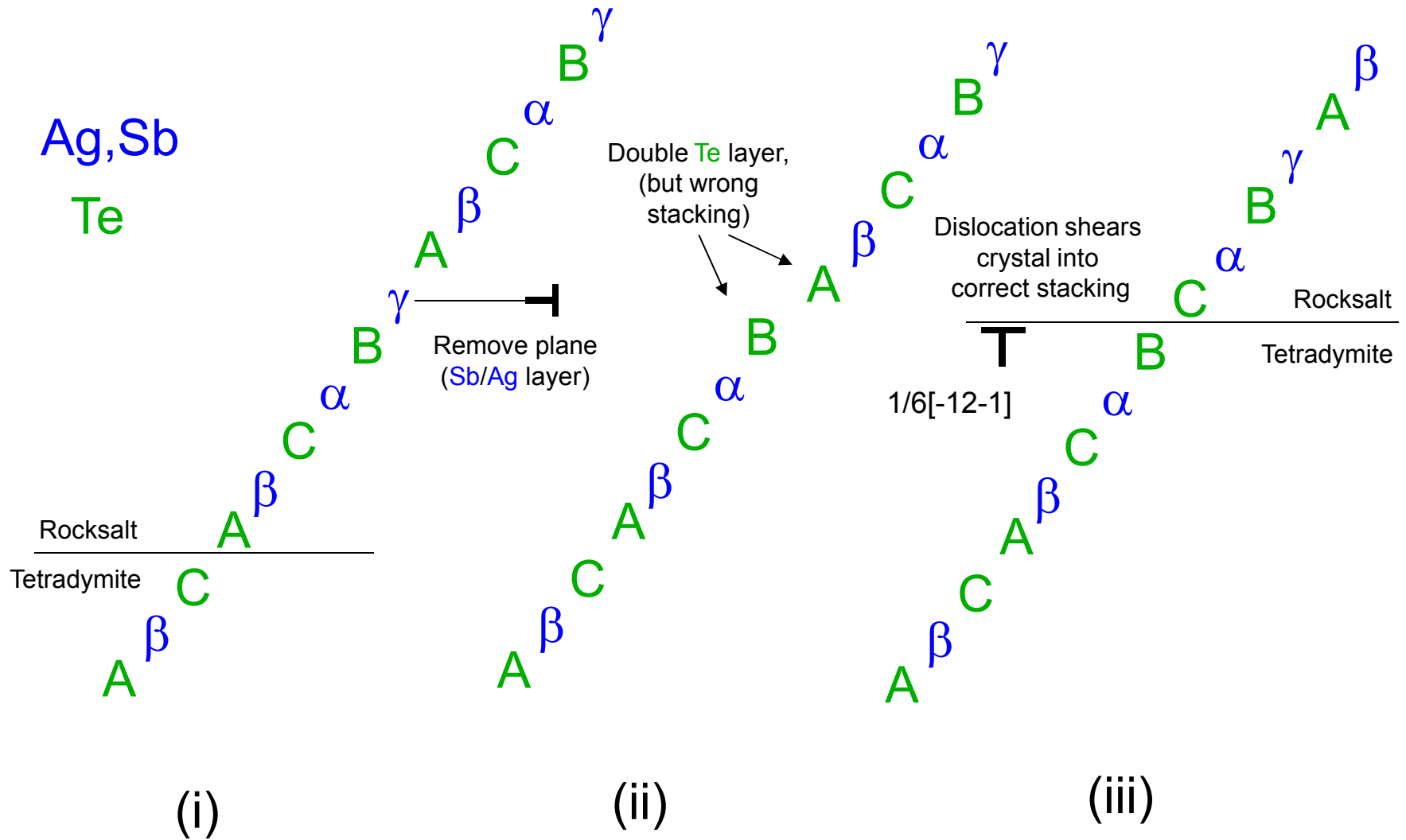
- mismatch of step heights.
- $|\mathbf{b}_n| = 0.3747\text{\AA}$

$$\mathbf{b}_\parallel = \frac{a_{cub}}{6} [\bar{1}2\bar{1}]$$

- Analogous to Shockley partial Dislocation
- $|\mathbf{b}_\parallel| = 2.48\text{\AA}$

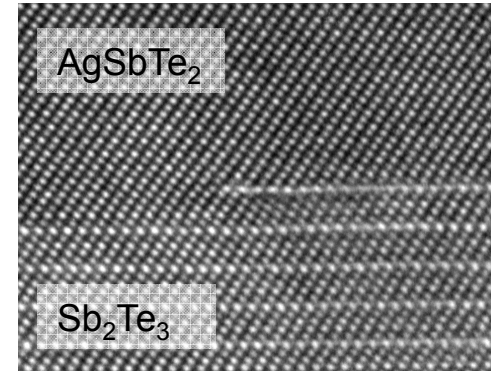
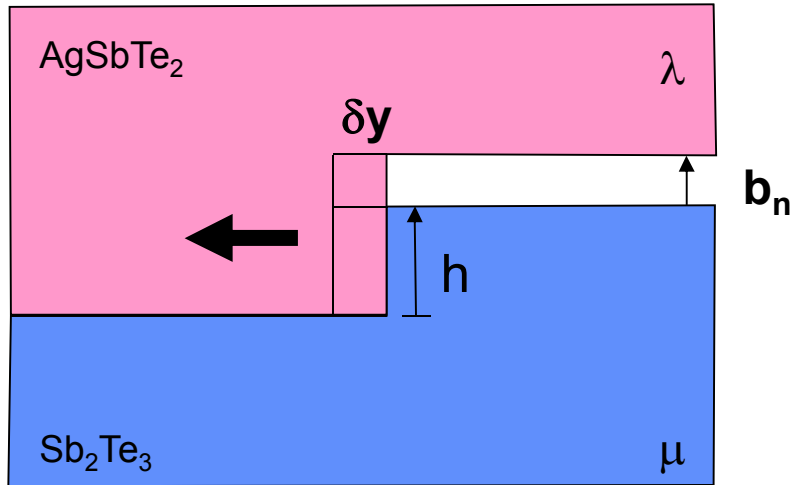


Schematic of Transformation Sequence



Defect properties give local mass flux required for transformation

Partition flux for defect motion into step and dislocation components



$$\frac{\Delta N_i}{L\delta y} = \underbrace{(\chi_i^\lambda - \chi_i^\mu)h}_{\text{step}} + \underbrace{\chi_i^\lambda b_n}_{\text{dislocation}}$$

Hirth & Pond, Acta Mat 1996

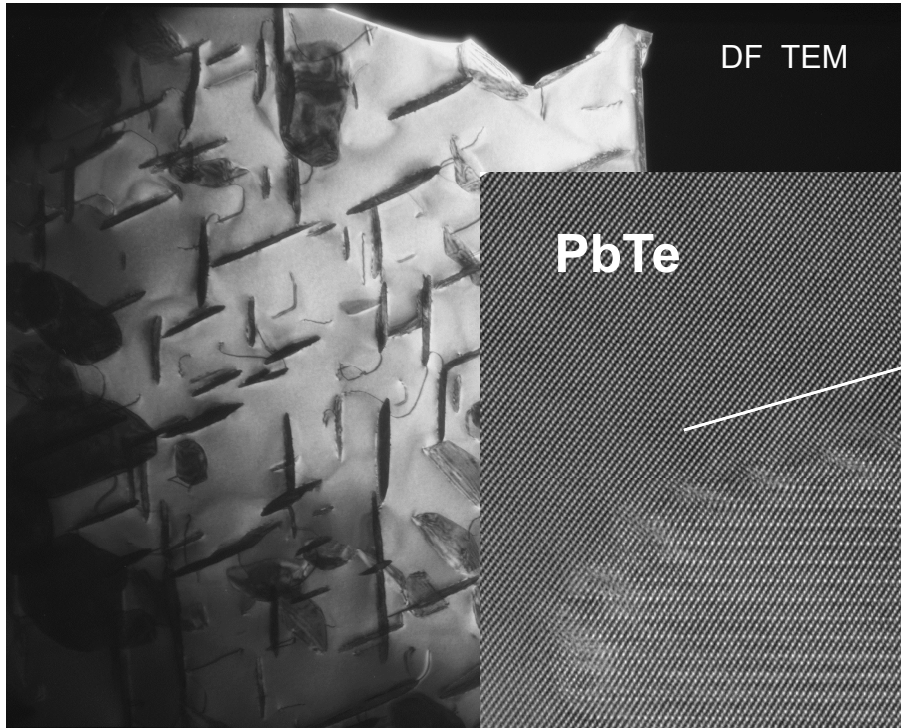
**Reject Ag and Incorporate Sb
in ratio of 3:1**

**Tellurium:
Step and Dislocation fluxes cancel.
No long-range Te transport required.**

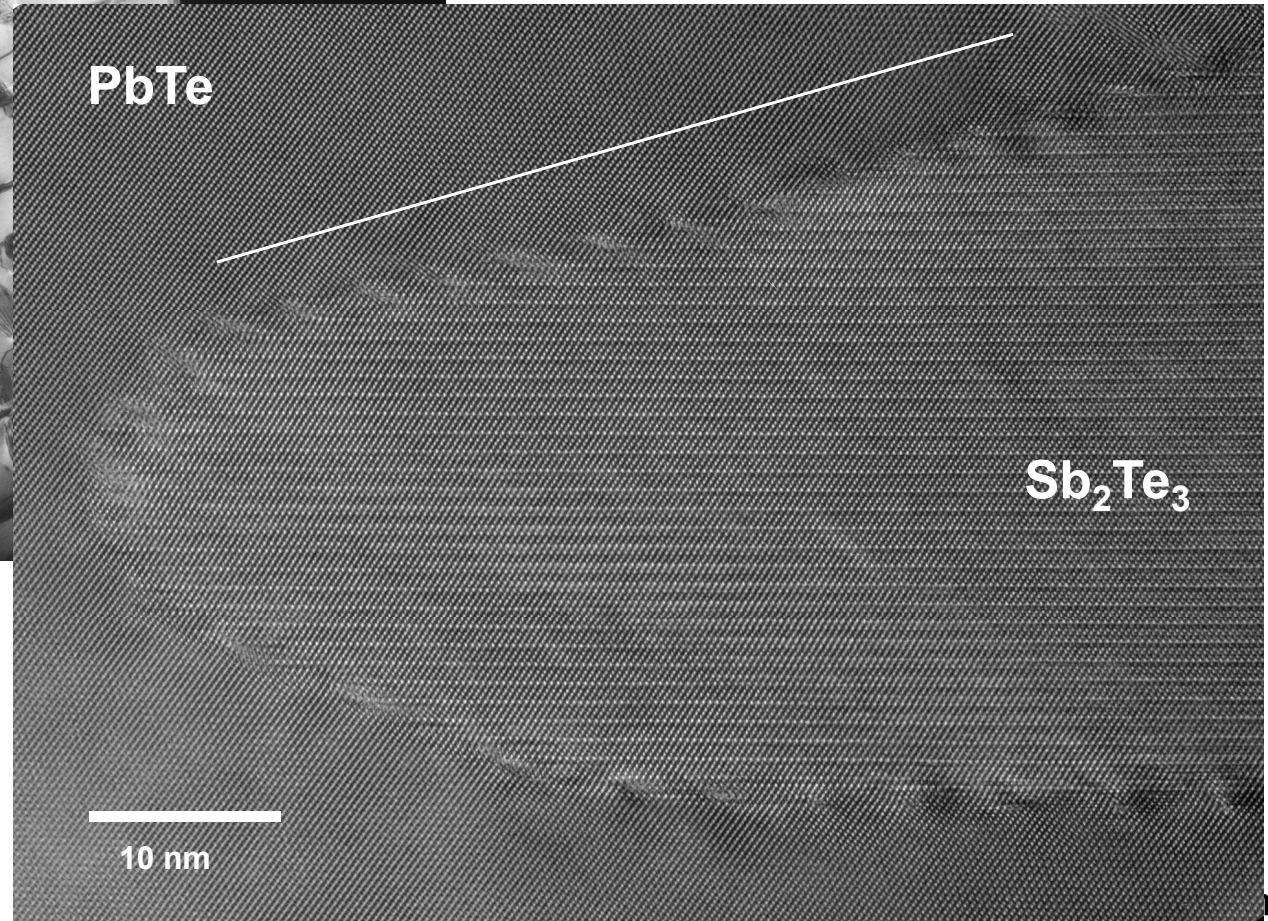
Species	Step flux (atoms/Å ²)	Dislocation flux (atom/Å ²)	Total flux (atom/Å ²)
Ag	$\frac{2 c_{hex}}{3 a_{cub}^3}$ +0.09043	$\frac{2}{a_{cub}^3}(\sqrt{3}a_{cub} - c_{hex}/3)$ +0.00334	$\frac{2\sqrt{3}}{a_{cub}^2}$ +0.09377
Sb	$\frac{2 c_{hex}}{3 a_{cub}^3} - \frac{8\sqrt{3}}{3 a_{cub}^2}$ -0.03459	$\frac{2}{a_{cub}^3}(\sqrt{3}a_{cub} - c_{hex}/3)$ +0.00334	$-\frac{2\sqrt{3}}{3 a_{cub}^2}$ -0.03126
Te	$-\frac{4}{a_{cub}^3}(\sqrt{3}a_{cub} - c_{hex}/3)$ -0.00668	$+\frac{4}{a_{cub}^3}(\sqrt{3}a_{cub} - c_{hex}/3)$ +0.00668	0

A system with larger misfit: PbTe/Sb₂Te₃

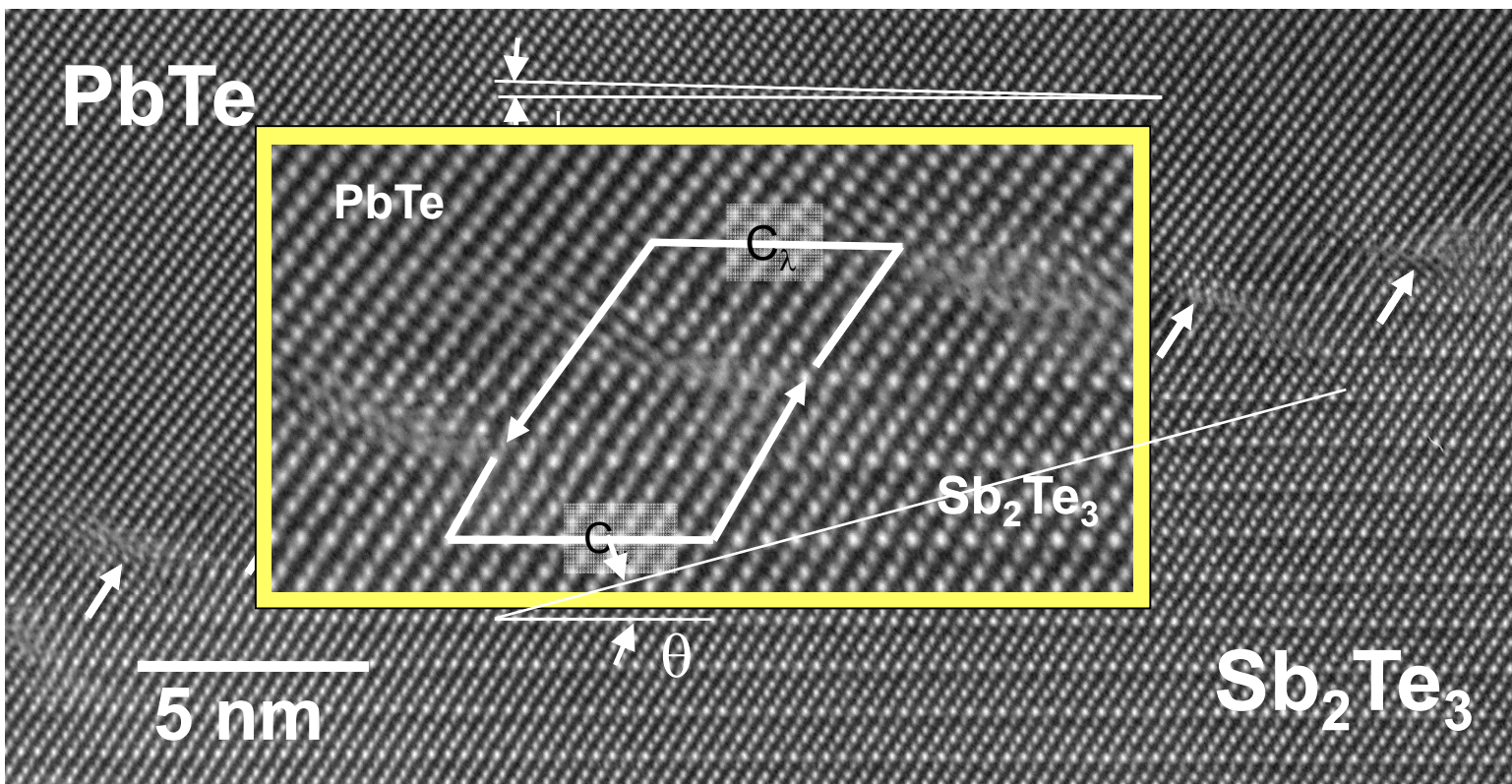
Sb₂Te₃ Precipitates in PbTe



AgSbTe₂(111)/Sb₂Te₃(0001)
Misfit: +0.79%



Inclined Section of interface Composed of Disconnections



HRTEM JEOL 4000EX

Circuit Analysis:

Defects identical to the “6/5” disconnections observed in $\text{AgSbTe}_2/\text{Sb}_2\text{Te}_3$

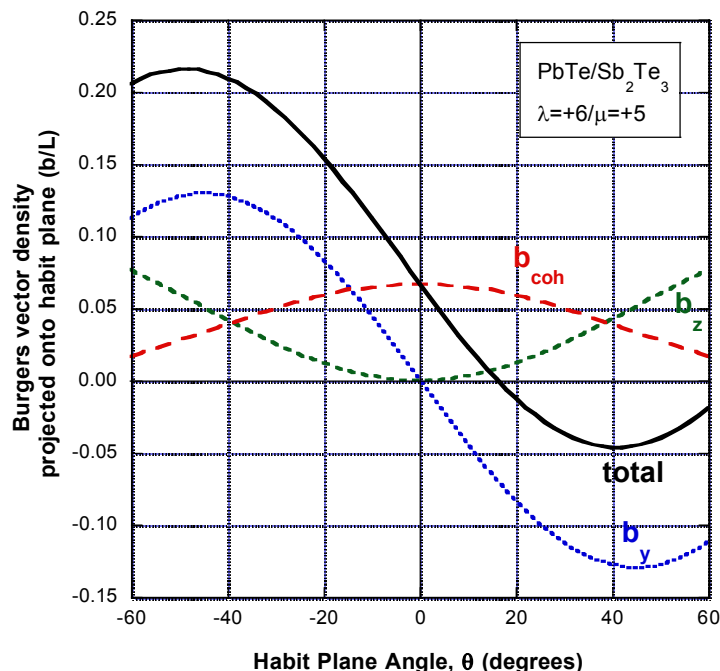
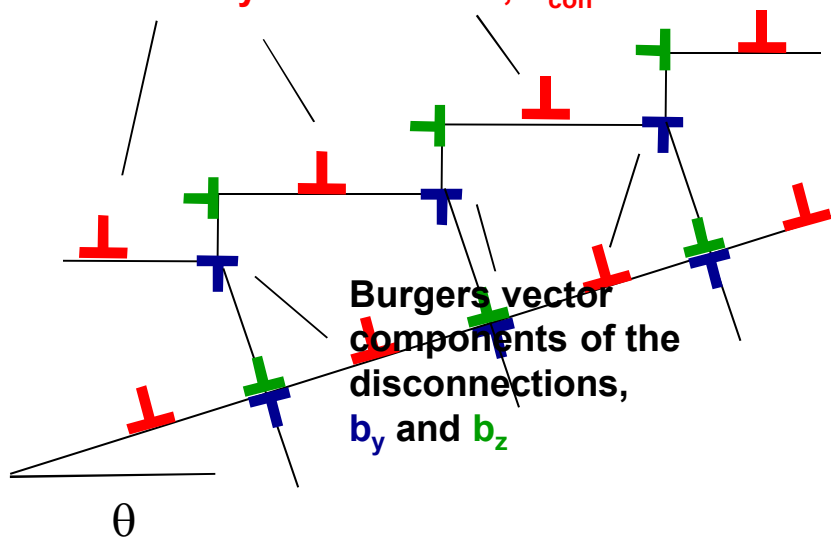
Interface Geometry:

Inclination: $\theta = 14.8^\circ$ Lattice rotation: $\phi = 1.1^\circ$ to 1.4°

Interplay between Misfit Accommodation and Interface Inclination

Project components on inclined interface plane

Adjust spacing to cancel ($\epsilon_{yy} = 0$)
 as "coherency" dislocations, b_{coh}



$$-\epsilon = (b_y \tan\theta + b_z \tan^2\theta)h^{-1} \quad \rightarrow \quad \theta = 16.2^\circ$$

Pond, Celotto, Hirth, Acta Mater. 2003

Out of plane \mathbf{b} components produce small rigid body crystal rotation,

$$\phi = 2 \sin^{-1} [(b_z \cos\theta - b_y \sin\theta - \epsilon h \cos\theta) \sin\theta / 2h] \quad \rightarrow \quad \phi = 1.7^\circ$$

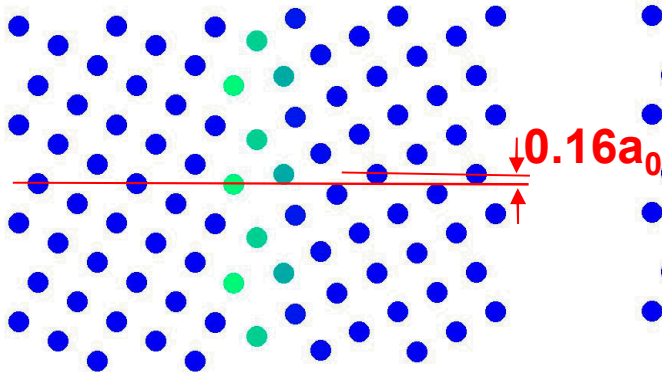
Disconnection spacing accommodates the (111)/(0001) coherency strain.

Summary

- **Analysis of interfacial defects provides insights concerning structure and mechanisms.**
 - Complex core structures for defects and grain boundaries.
 - Junction-defect interactions.
 - Mechanisms underpinning phase transformations.
- **Interfacial defects: bridge between atomistic scale observations and simulations and mesoscale scientific understanding**
 - Establishing the defect geometry (step and Burgers vector) is critical.

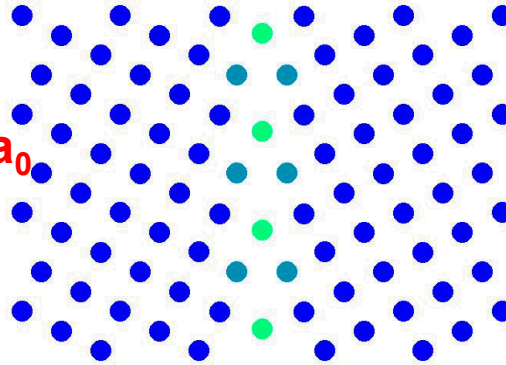
$\Sigma=5$ {310} Structures with different Potentials

Asymmetric



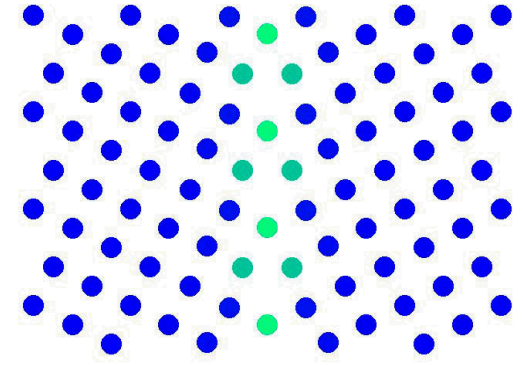
Potential: Chamati, 2006

Symmetric



Potential: Mendeleev, 2003

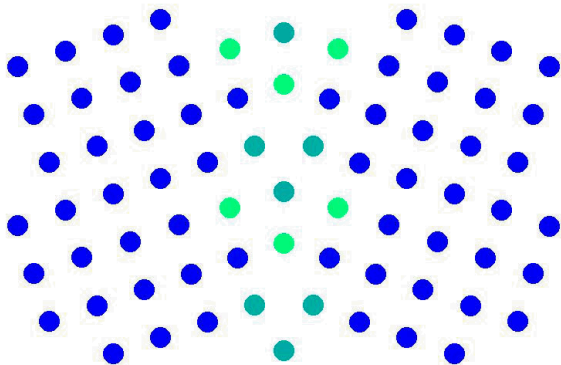
Symmetric



Potential: Proville, 2012

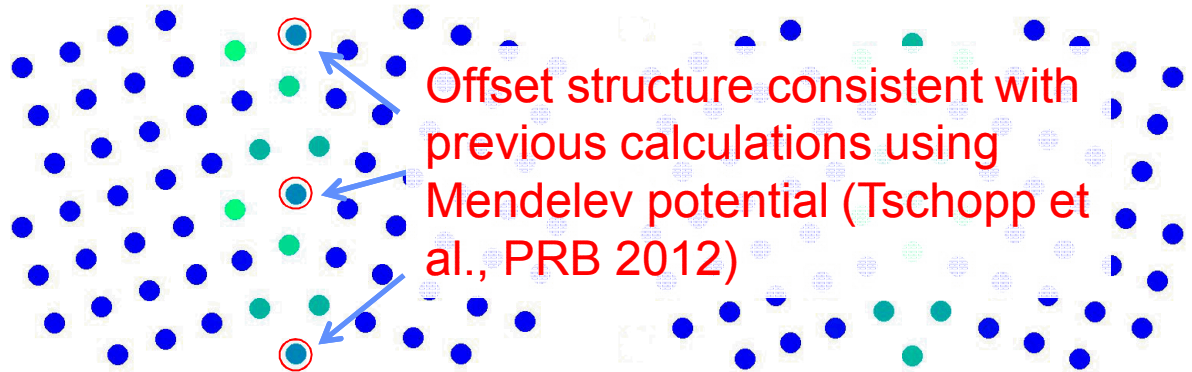
$\Sigma=5$ {210} Structures with different Potentials

Symmetric



Potential: Chamati, 2006

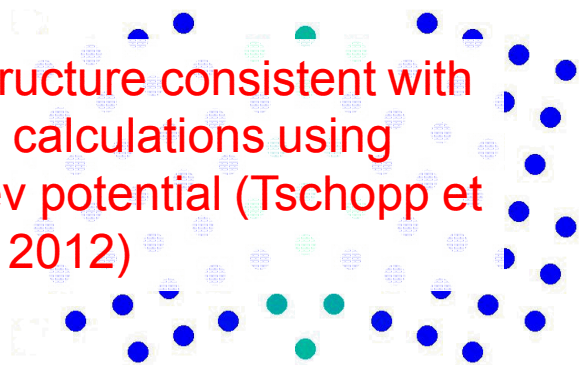
Asymmetric



Offset structure consistent with previous calculations using Mendeleev potential (Tschopp et al., PRB 2012)

Potential: Mendeleev, 2003

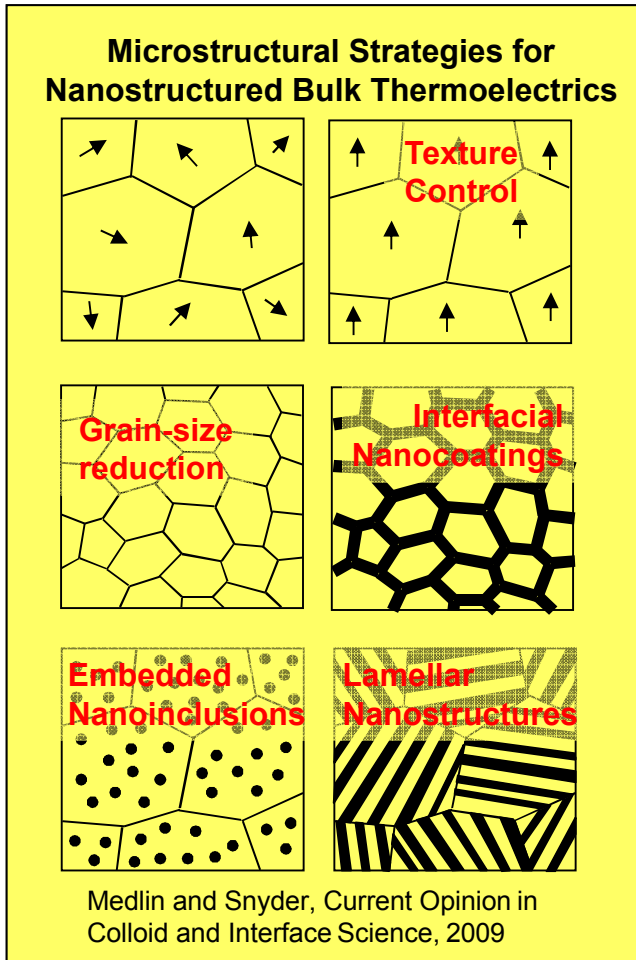
Symmetric



Potential: Proville, 2012

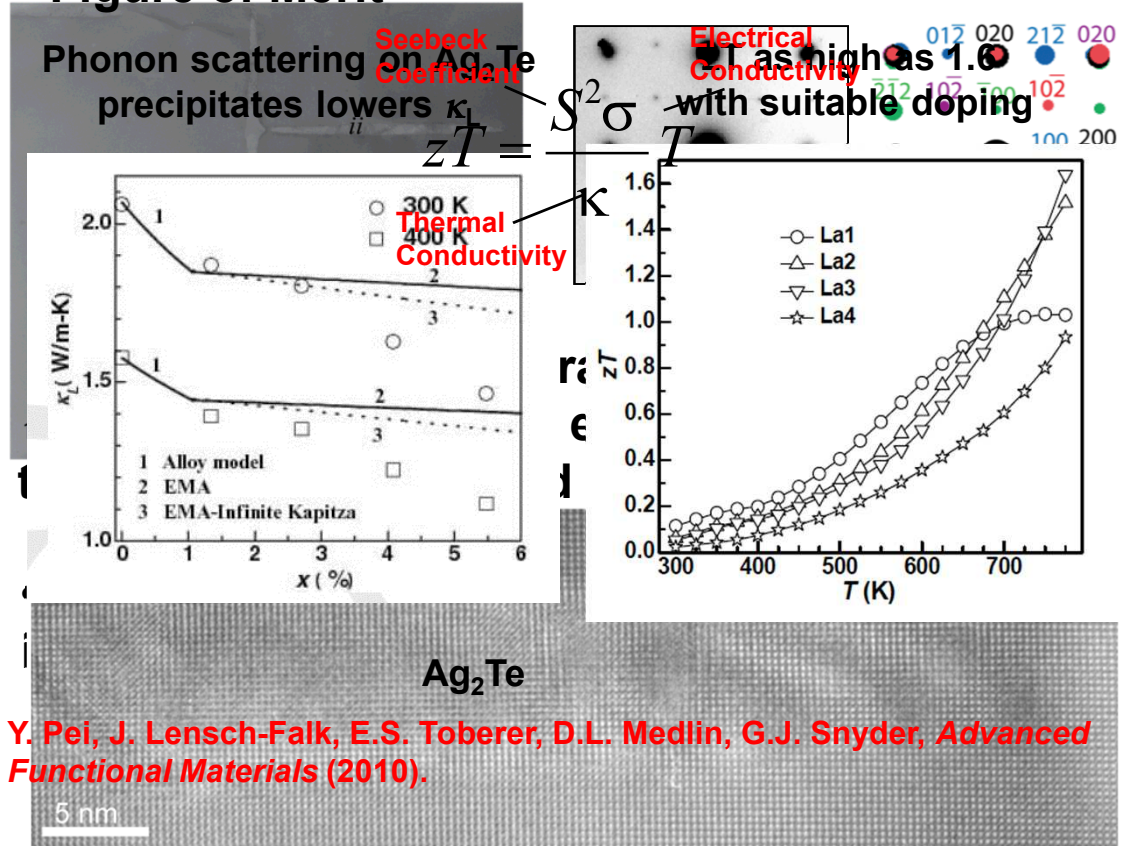
Atoms shaded by centrosymmetry parameter

Bulk Thermoelectrics: Control of Microstructure to Improve Performance



TE Energy Conversion Efficiency: PbTe Example: Ag₂Te nanoprecipitates

Figure of Merit

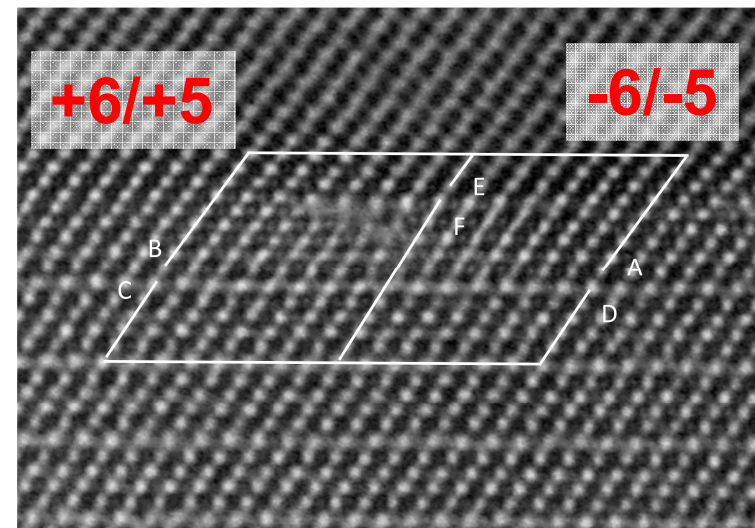
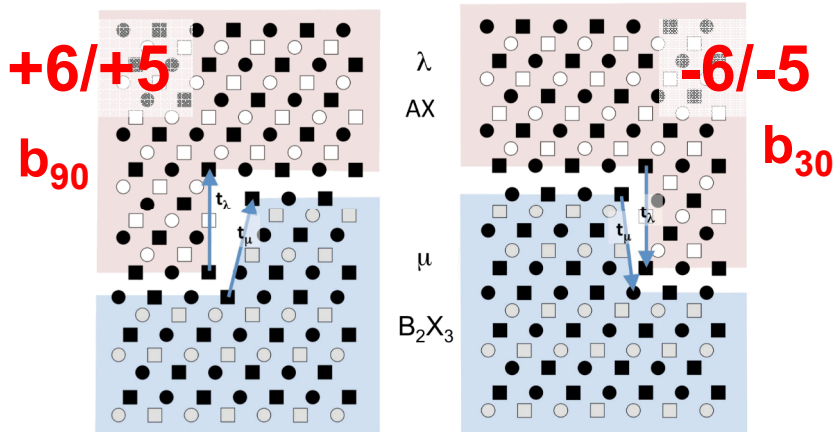
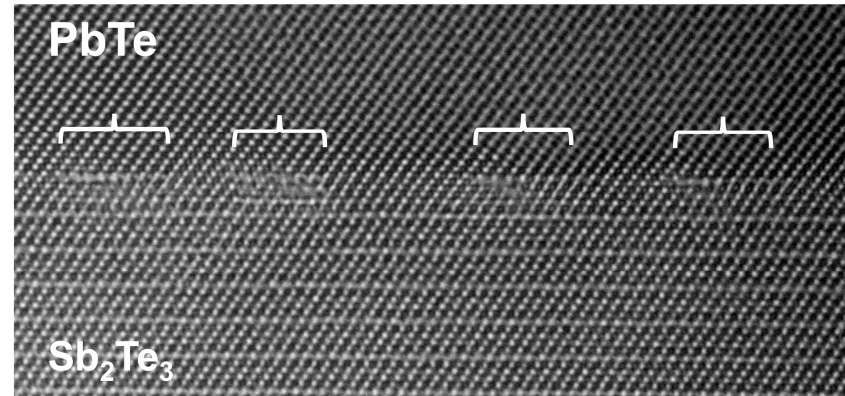
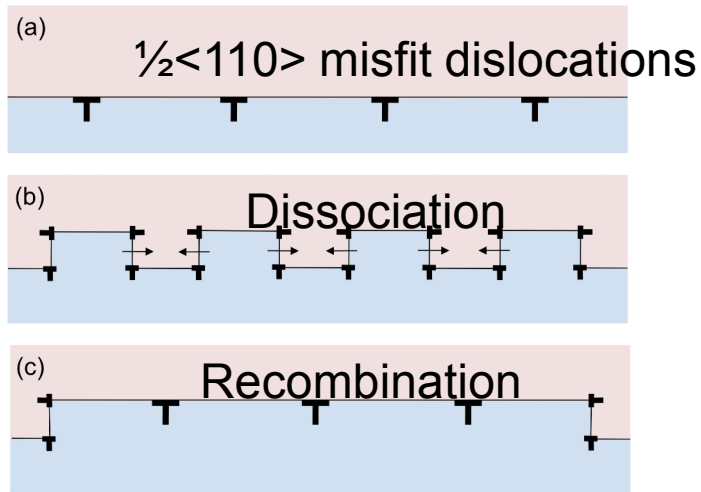


Y. Pei, J. Lensch-Falk, E.S. Toberer, D.L. Medlin, G.J. Snyder, *Advanced Functional Materials* (2010).

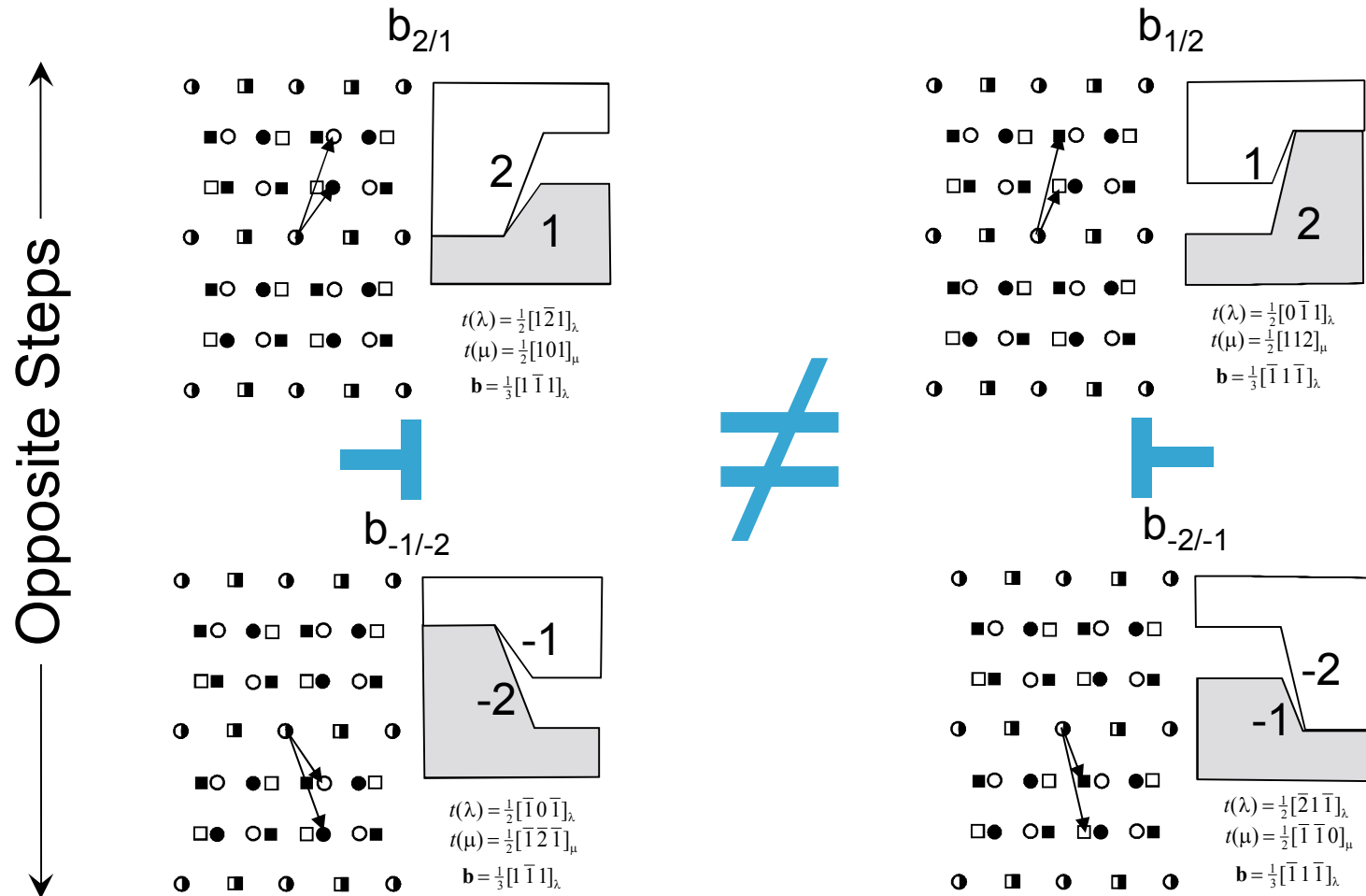
J. Lensch-Falk, J. Sugar, M. Hekmaty, D. Medlin, *Journal of Alloys and Compounds* (2010)

How might these defects form?

Dissociation of $\frac{1}{2}\langle 110 \rangle$ misfit dislocations
at flat sections of interface into disconnections



Variants of the $1/3\langle 111 \rangle$ Disconnection



Classical Distinction between High and Low Angle Boundaries

